Diagnostic of an RF Atmospheric Pressure Plasma Jet: Wounds treatment application

Sylvain Iséni

Eindhoven University of Technology
Department of Applied Physics
Elementary Processes in Gas discharges

Diagnostic of an RF Atmospheric Pressure Plasma Jet

Sylvain ISÉNI

June 2011 EPG 11-08

Under supervision of:
Dr. ir. BRUGGEMAN Peter
PhD Stud. HOFMANN Sven

Technische Universiteit Eindhoven University of Technology

Where innovation starts

Sylvain ISÉNI

sylvain.iseni@etu.univ-orleans.fr

Engineering & Master Student

POLYTECH' ORLEANS

FRANCE

Diagnostic of an RF Atmospheric Pressure Plasma Jet

Wounds treatment application

Elementary Processes in Gas Discharges

January 31st - July 1st 2011

Project heads: HOFMANN S., PhD Stud., *s.hofmann@tue.nl*
VELDHUIZEN van E., dr.ir., *e.m.v.veldhuizen@tue.nl*
BRUGGEMAN P., dr.ir. *p.j.bruggeman@tue.nl*

Contents

List of Figures

List of Tables

Acknowledgements

I would like to start my report with many thanks especially to Dr.ir. Eddie van Veldhuizen and Prof. Laïfa Boufendi and prof.dr.ir.Gerrit Kroesen who organized this exchange between EPG and Polytech'Orléans. It is such opportunity for me to go abroad for the first time and discover so many things here in the Netherlands. I am grateful towards Dr.ir. Peter Bruggemann and PhD. Sven Hofmann to supervise my work and for all the knowledge that I learn from them. I would like also to thank them for their help and their availability because they always want to answer my questions. It happened sometimes very late at night, and they always answer by e-mail even in the week-end to allow me to continue my work. This means that they also are ready to lend a sympathetic ear and I would like to thank them again for that. It was such big chance to work with them and it is definitely one of my best student experiences! This project is a huge opportunity for me to develop my skills in plasma physics and particularly about the plasma jets.
More generally, I thank all the people who work at EPG. I also would like to thank PhD. Christopher Vasko for all the discussions that we had in the lab, especially during the long experiments of spectroscopy measurements. It was a real pleasure to talk with him and very great to share some part of his setup to allow me to continue my work in the lab.
I hope that we will meet again...

Abstract

Plasma physics is a very multidisciplinary because we have to use a lot of fields such as electromagnetism, chemistry, thermodynamics, electrical sciences, atomic and molecular physics, fluid mechanics, vacuum technology .... If we add to the above also plasma diagnostics, we also have to consider optics, mechanics, optronics and electronics. few years now, plasma physics has entered the field of medicine. This evolution is so important that some scientists compare the plasma medicine application to the development of the laser technology a few decades ago. This report contains the results, analysis and discussion of a diagnostics study of an Argon and Helium RF atmospheric pressure plasma jet. We present measurements of dissipated power in the plasma, the emission spectroscope and the gas temperature of the jet. In order to create more reactive species which could be beneficial for biomedical applications, we add small amounts of Nitrogen or Oxygen to the jet. The influences of these mixtures are investigated and the results are discussed. To approach to the future applications conditions, some tests are performed during which the plasma interacts with saline solutions or distilled water and investigated. This leads us to compare all the results together in order to get some conclusions about the power, gas temperature and emissions.

Chapter 1

Atmospheric Pressure Plasma Jet

1.1 Brief overview of atmospheric pressure plasma jets

Plasma is the fourth state of matter. We can find it in space, but it is also possible to find it on Earth even if it is difficult especially because of the surroundings. The plasma state is not very well known by people, but one should know that a lot of products are made by using manufacturing plasma processes. Usually, many of these processes are done in a plasma reactor where the pressure is around one to thousands million times lower than the atmospheric pressure!

Nowadays, many groups of scientists are really interested to design new kinds of plasma sources such as the atmospheric pressure plasma jets (APPJ). Medicine-driven, the development of this plasma generation is extremely important in order to launch new medicine treatments. This is one of the main reasons why research groups are mostly interested by this generation of plasmas. But the applications of the APPJ will be developed in another part of this report.

The main difference between the plasmas which are created within reactors and the plasma jets is the pressure. While common plasma sources are operated at low pressures, the plasma jets are operated at atmospheric pressure. This enables us to use some plasma proprieties for treating surfaces without using a specific vessel with a high vacuum chamber. For example, the facilities could be cheaper because you do not need a pumping system. The other main characteristic of this kind of plasma is the heavy species temperature of the plasma[1]. That is to say the electron temperature which is directly linked to the electron energy is much higher than the ion and neutral temperatures, so than the gas temperature: $T_e >> T_i \approx T_n \approx T_g$. This is the reason why APPJ are also called Atmospheric Pressure Non-Equilibrium Plasmas because of the non-thermodynamic equilibrium[2]. This property of the APPJ is interesting too and allows using it with the materials which cannot withstand excessive heat. For instance, it enables us to treat polymers surfaces or tissues in order to treat human wounds in the future.

Before to deal with specific proprieties or characteristics of the APPJ, it is important to know that the APPJs are a specific group of plasmas. In the group, there are different kinds of APPJs and it's possible to sort them to different criteria but it is not the goal of this paper. One way to generate an APPJ is to use a needle which plays the part of one electrode; this component is able to generate an electric field which can ionize the gas. The plasma is enhanced by using a gas flown at rates that are several standard liters per minute (slpm). The presence of a gas

[1] the plasma temperature refers to the ion and neutral temperature and not the electron temperature; we could also say gas temperature, but the plasma is not a gas strictly speaking

[2] A system is in thermodynamic equilibrium when it is in radiative equilibrium, mechanical equilibrium, thermal equilibrium and chemical equilibrium. In this case, the system is not changed if there is not exchange with its surroundings.

flow around the needle *blows* the plasma outside and creates a jet of a few millimeters to a few centimeters.

1.2 Devices and applications

The APPJs have been studied for a few years by several research teams around the world. The jet at the end of the device is also called plume. In order to generate this plasma, you need to give some energy to the gas for ionizing the molecules inside. Fortunately, there are many possibilities to give the energy which is why there are different kinds of devices.

1.2.1 A piece of theory: the Paschen's Law

All the devices which will be introduced and even more are designed in order to meet Paschen's Law. This law characterizes the conditions which can induce a breakdown voltage and create the plasma. The breakdown is the result of a high ionization rate of the molecules and by this way it is possible to initiate the plasma. The equation 1.1 describes the reaction where the pressure p [Torr] and d [cm] the gap distance between two electrodes are the main parameters. V_b is the breakdown voltage. The γ parameter is the second Townsend coefficient or second emission coefficient. Its value depends of the electrode's nature. C_1 and C_2 are two constants which depend of the gas. The units are cm^{-1} $Torr^{-1}$ and Vcm^{-1} $Torr^{-1}$ respectively.

$$V_b = \frac{C_2 \cdot pd}{\ln\left(\frac{C_1 \cdot pd}{\ln\left(1 + \frac{1}{\gamma}\right)}\right)} \tag{1.1}$$

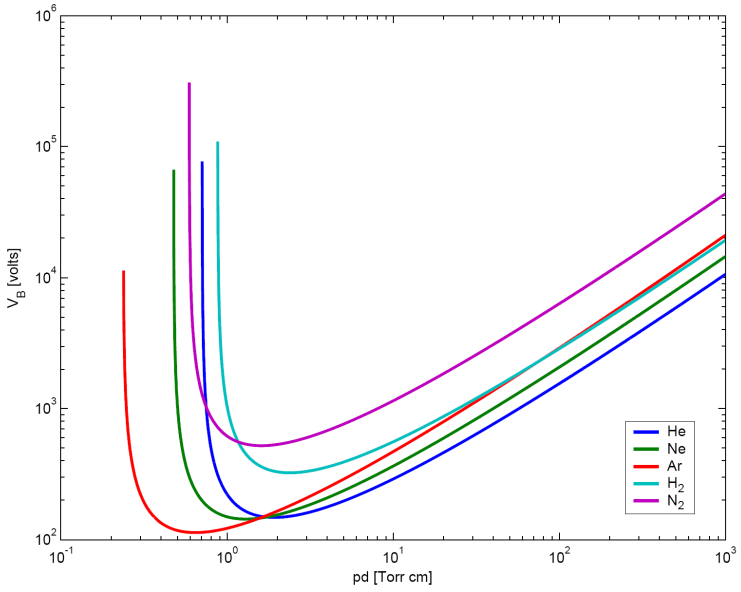

Figure 1.1: Paschen curves for different gases.

It is possible to plot a graph of the Paschen's formula for each gas. Figure 1.1 shows the curves for different gases. We can see that each of them gets a minimum breakdown voltage for a specific value of the pressure times the distance between two electrodes. In the case of the APPJ, the pressure is fixed by the atmospheric pressure which is high for the plasma physics. Thus, the breakdown voltage is decreased by decreasing the gap at the electrodes. Typically a few millimeters, but it depends of the applied voltage. The optimal parameters can be found by the relation 1.2 according to the nature of the gas.

$$V_{b_{min}} = C_2 \cdot \frac{e}{C_1} \cdot \ln\left(1 + \frac{1}{\gamma}\right) \tag{1.2}$$

1.2.2 Pulsed Direct Current Driven power supply

One of the solutions for creating a plasma is with using Pulsed DC power. The usable voltage range can go up to several kV and the pulse width ranges from a few nanoseconds to microseconds. The repetition rate is usually a few kHz. The general shape of this kind of device uses two planar electrodes. The gas mixture is injected between both. This setup is similar to a Dielectric Barrier Discharge (DBD) which is used to avoid the arcs inside the current which goes through the two electrodes. DUAN *et al.*[6] measure that the gas temperature at the end of the tube is between 40 to 85 °C and the range rate in the gas flow is 1 slpm to 3.5 slpm. Förster *et al.*[1] have developed a plasma jet which uses also a DC pulse. The setup is a bit different because they use a ring around the tube which is connected to the a high voltage; typically 15 kV with a 600 ns pulse width at a repetition rate of 25 kHz. They also use a needle inside the tube which is grounded. The gases which are usually used are Argon, Helium, Nitrogen or some mixture of these with Oxygen. A possible application is to use this plasma jet to treat surfaces, *e.g* to increase the surface wettability of wood.

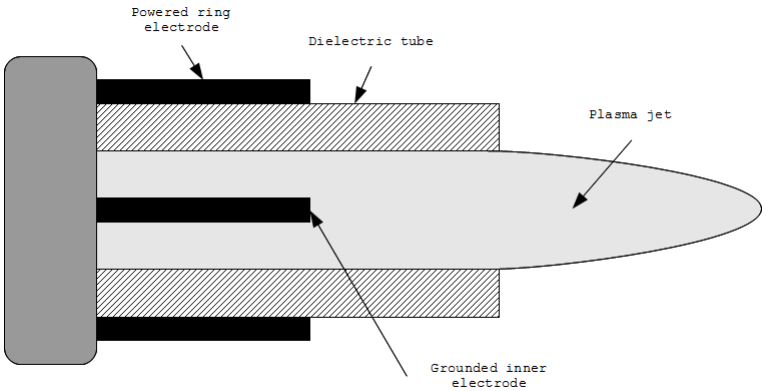

Figure 1.2: Schematic of the APPJ developed by Förster *et al.*[1].

Laroussi and Lu[7] developed another device which can generate a plasma jet. It uses a similar power supply as the two previous one but the configuration of the device is a little different and it will be not developed in this report but people who are interested by it could refer to the following paper [8]. The main parameters of this apparatus are the voltage amplitude which is roughly 10 kV, pulse width variable from 200 ns to DC and the repetition rate up to 10 kHz. The temperature of the jet is close to 290 K and the average length of the plume is 5 cm. At the moment, the more famous application of this device is the sterilization of infected objects. You can see on the figure 1.3 the result of a test where the petridishes were treated by the *Helium Plasma Pencil*. The

petridish on the top is the reference and all the dishes contain the same amount of *Escherichia Coli* bacteria. The left dish was exposed for 30 s to the jet and the right dish was exposed for 120 s. We can see an area without bacteria in the middle of the petri-dishes that means that the plasma jet treated and killed the bacteria in these areas.

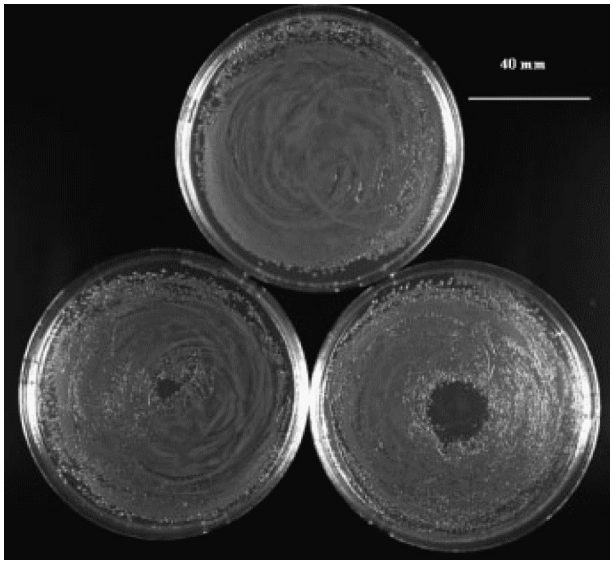

Figure 1.3: Results of the test of sterilisation with the *Plasma Pencil* from *Laroussi and Lu*[2].

1.2.3 Alternating Current Driven power supply

Another means to drive a plasma jet is to use an AC-power supply. These types of devices are much closer to a Dielectric Barrier Discharge concept due to the facing presence of two large electrodes separated by a dielectric layer. As Teschke *et al.*[9] and Cheng *et al.*[3] noticed when they test their own plasma jet, this kind of device produces plasma bullets as the DC pulse. The order of magnitude of the bullets velocity is guessed 15 $km \cdot s^{-1}$. A sinusoidal high voltage of a few kV at the frequencies in the 5 to 50 kHz range is applied and a gas flow is 16.5 $m \cdot s^{-1}$. It is reported that the temperatures which were measured are in the 300 - 490 K range. The application of this kind of plasma jet is to process material surfaces like wood. Thus, the authors claim that it's possible to treat polymer films in order to increase its wettability. The figure 1.4 shows an example of AC-driven plasma jet developed by Cheng *et al.*. It is designed to use voltages of 30 to 80 kV at the frequencies range from 6 to 20 kHz.

1.2.3.1 Radio Frequency Driven Power supply

One of the most used means to create a plasma jet is with Radio Frequencies (RF). In this part we explain briefly how it works and where this kind of jet is used or plan to be used. The APPJ is usually made with a tube and a metal needle inside which is one of the electrodes[3]. The electrodes could also be a ring around the tube instead of a needle. The inside electrode is linked to the RF power supply when the outer electrode which could be a simple ring of copper is grounded. Sometimes you could find some setup without this second grounded

[3] A description of the device is not done in the sections 1.2.2 and 1.2.3 because it is roughly the same as the following description

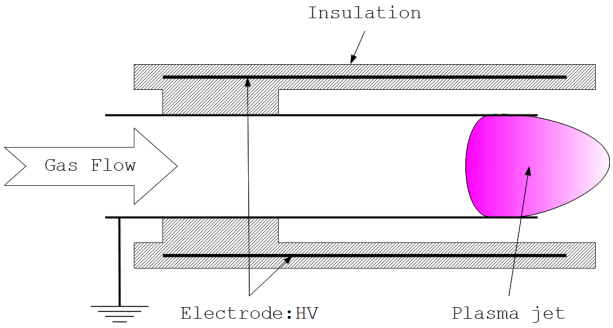

Figure 1.4: Schematic of the plasma jet device developed by Cheng *et al.*[3].

electrode. In this case, the air within the room is the second electrode. This difference determines some aspects or properties of the plasma jet that is why it is really important to precise it when you describe the configuration. The power supply is connected to the central electrode and the frequency is fixed at 13.56 MHz. A match box is used in order to reduce the reflective power from the plasma to the generator. This phenomenon is due to the capacitive characteristic of the APPJ. Others details will be developed further, especially in the chapter 4. The gas flow is roughly between 1 to 25 slpm and depends on the design of the device. The gas temperature of the jet depends on the gas mixture, applied power, gas flow and is reported to be in between 300 K to 500 K.

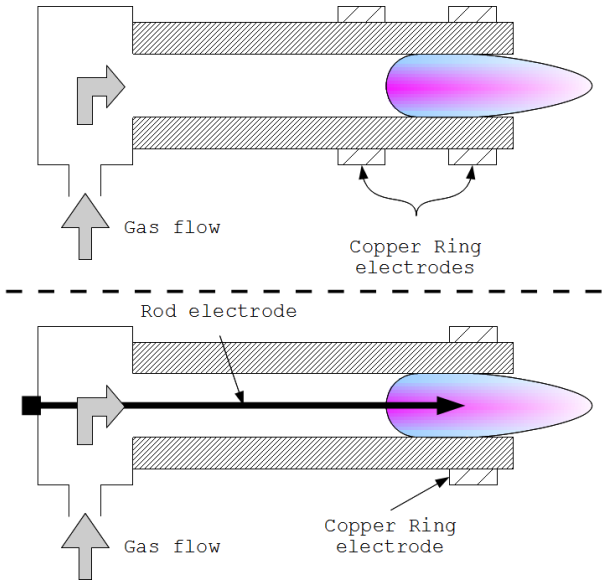

Figure 1.5: Schematics of both versions of the RF APPJ from Foest *et al.*[4].

About the applications, Koinuma *et al.*[10] claim that it is possible to process materials with an Argon plasma, Helium plasma with a mixture of both. For instance, they treated a vulcanized rubber compound to improve its adhesion properties. They also etch a piece of silicon by using a mixture of helium with 1% of CF_4. It was also done for depositing silicone dioxide on a silicon wafer using tetramethoxysilane, TMOS, carried with an Ar and a di-hydrogen mixture. The authors also claim that it is possible to deposit others materials layers such as TiO_2. Of course, there are various processing applications especially in biological field. One of the best examples is sterilization of bacterium. An experiment was done by Herrmann *et al.*[11] and they published the results in 1999 where we can learn that 90% of the initial *Bacillus globigii* spore population were killed after an exposure of

4.5 s with a plasma jet which used air as operating gas. It is also possible to etch SiO_2, tantalum, kapton and tungsten. Tu *et al.*[12] precise that the etching rates achieved were 8 $\mu m.min^{-1}$for kapton, 1.5 $\mu m.min^{-1}$for SiO_2, 2 $\mu m.min^{-1}$for tantalum and 1 $\mu m.min^{-1}$for tungsten. Some other research of Stoffels and co-workers[13] has already done some experiments with their plasma jet with tissues. There are a lot of very interesting results which show that the APPJ are really useful especially in biomedical fields. It is because of the recent experiments and the promissing results that the APPJ are widely investigated by unions research groups.

1.3 The RF-driven APPJ at EPG

In this section, we are going to introduce the APPJ which is used at EPG. First of all, it is an RF-driven plasma jet. As it was said in the previous section, this kind of plasma is a capacitive couple device. Typically, the first electrode which is connected to the generator is a needle which is fixed inside a small tube where the gas is flowing. The RF generator is connected to the needle electrode. Due to the electric field between the needle and the tube a lot of free electrons are accelerated and enter in collisions with the molecules of the background gas which is in the tube. In our case, the second electrode which should be grounded is outside a few millimeters after the tip of the needle. This second copper electrode is often removed. Thus, there is no physical electrode and the theory says that in this case the second electrode is the air within the room. Since we removed the second electrode, we cannot say that the air is grounded because it is at the floating potential. The collisions from the electrons excite the molecules where some of them are ionized due to the inelastic collisions. In this step, the electrons are created by the RF field which accelerate the electrons and lead to the ionizing collisions too; this is the avalanche effect which is controlled by the energy balance. As a result, a lot of reactive species like ions, atoms, molecules and free radicals can be created. This is roughly the mechanisms which enhance the plasma jet. Figure 1.6 shows the dimensions of this device and some additional details.

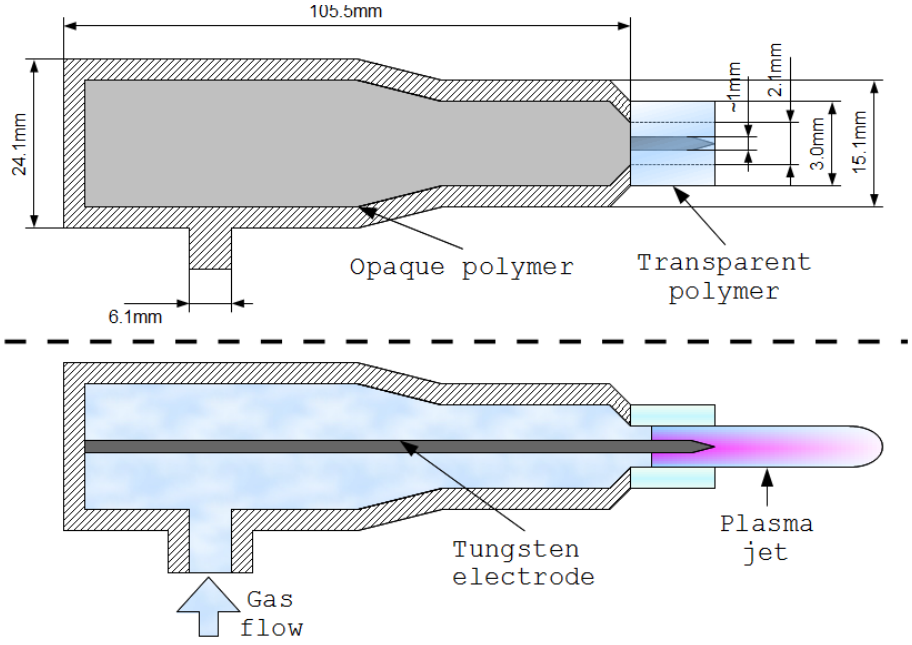

Figure 1.6: Schematics of the APPJ which is used at EPG.

1.4 Basic setup and materials

In this section, the setup is introduced as well as all the components for the APPJ device.

- The power supply is a generator from Agilent Technologies© 33220 A at 20 MHz or the 33120 A at the maximum frequency of 15 MHz. It is coupled with an amplifier.
- The amplifier is from Amplifier Research©.Model 57AP250, signal output is 75 W at 5 to 250 MHz range.
- Two mass-flows Delta smart II from Brooks Instruments©. Each of them is controlled by a digital mass-flow-controller, reference 0254. One flow meter is calibrated for Helium and can be used for flow rates from 0 to 10 000 sccm[4]. The other is made for using Oxygen in the range 0 to 300 sccm.
- Oscilloscope DSO-X 2024A made by Agilent Technologies©, maximum frequency 200 Mhz at 2 GSa/s.
- Voltage probe Tektronix© Tek P5100 is used. The multiplying coefficient is 100 times and the maximum peak value which is taken is 2 500 V at the maximum frequency of 250 MHz.
- Current probe is a Pearson©, model 2877.

As it is a capacitive plasma, it is required to use a matching box in order to adapt the impedance between the generator-amplifier and the plasma otherwise the power coupling with the plasma will be very inefficient. The matching box is just a single coil yet because it is easier to measure the power dissipation of the plasma. Otherwise, a L type or a π type box are usually made of a various capacitor and a self-inductance. In our case, we adjust the signal frequency to maximize the power coupling into the plasma. The figure 1.7 illustrate the whole basic setup that we use for our experiments.

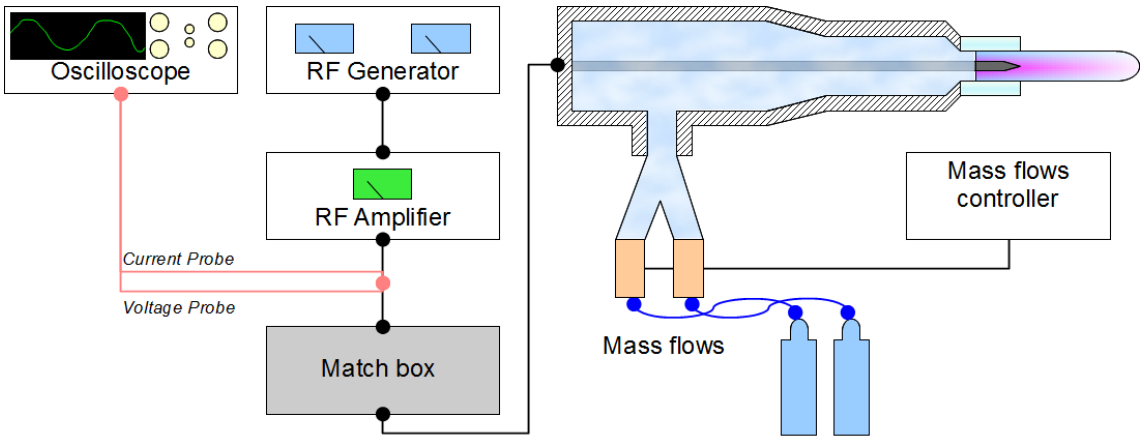

Figure 1.7: The basic setup of the APPJ at EPG

[4]This is the theoretical range from the manufacturer but we note that the minimum value is around 2% of the maximum value. In this case, the minimum value is 200 sccm.

1.5 Main parameters and experimental objectives

There are a lot of factors which can influence the plasma jet. The used gases and the gas flows but also the power supplied to the plasma which is controlled with the generator. Finally, we could mention the gas flow inside the tube which seems to drive the outflow of the plasma. We can weigh up that these parameters are under control by the experimentalist and could call them *explicit* parameters because we can fix them easily. On the other hand, there are some kinds of factors which are more difficult to drive. For example, the amounts of impurities like Nitrogen or Oxygen. The variation of concentration of these species can change the characteristics of the plasma like the temperature, the radiation or merely the shape of the plasma plume. In those cases we can call these factors, *implicit* parameters because their control is less intuitive. The table 1.1 summarizes all the parameters that we have to take into account for the further experiments.

Parameter type	Factor(s)	Unit(s)
Gas flow	Ar / He	slpm
Power	Voltage / Current	V . A
Impurities	Nitrogen / Oxygen	sccm
2^{nd} Electrode	grounded / present / absent	$\varnothing$

Table 1.1: Main factors which can influence significantly the plasma characteristics

Main factors which can influence significantly the plasma characteristics are investigated in this report. The APPJ is produced with two different kinds of rare gases, which are Argon and Helium. Moreover, to investigate the influences of impurities of the air, small percentages of N_2 and O_2 are added. The investigations are based on the analysis of optical emission spectra from the plasma jet. We also look into macroscopic effects and optical appearance of the jet by taking pictures of the plume with a CMOS-camera. It is also important to get the gas temperature for different gas mixtures. The power investigation is also necessary to understand some properties of the plasma and could give information about the reactivity of the plasma. These points will be presented in the following chapters.

Chapter 2

Influence of the Impurities in the Argon and Helium APPJ

Before being scientists who are interested by the plasma physics, we are humans being. That is to say that we are used to use our own senses especially eyesight. Fortunately the APPJ radiations are visible that is why we started the experiments using a CMOS-camera in order to take some pictures. The aim of this chapter is to report some observations which can help for further investigations.

2.1 Pure Argon and Helium plasma jet

Usually, Argon is used because in a vacuum reactor, it is easy to get a plasma discharge. Argon is also a noble gas that means that it is very stable and the Argon atoms do not react easily with the other species. Argon and Helium are also easier to ionize than gases like O_2 or N_2 and the mechanisms of interaction between Ar or He and other species are well known for high pressure plasmas. This kind of plasma is generated at the atmospheric pressure and most of the time in open air. It is also the same reason why we use Helium. Due to their electronic configuration which is full, both cannot have a covalent bond but they merely transfer their energy to the other molecules in order to ionize or break their bonds.
Moreover, different publications show that especially these kinds of gases are able to give very good results for plasma medicine applications. However there have been a lot of things to investigate because this field of the plasma physics is quite new.

2.2 Impurities: Nitrogen and Oxygen

One of the aims of the APPJ is to create radical reactive species like OH, O_3, NO, O and N_2^+ in order to treat wounds. It may be possible to produce them with a pure Argon or Helium plasma jet, but the amount could not be enough for some specific applications. The plasma also can be unstable or the gas temperature too high. That is why we do some experiments with Argon and Nitrogen or Oxygen in a small ratio. By this way, we can

create more species and change the properties of the plasma which might be better for specific applications. The ratio used of impurities is set between 0.7% to 2.5%. Table 2.1 gives the different ratios that we use for all the experiments.

Concentration (%)	0.7	1.0	1.3	1.6	1.9	2.2	2.5

Table 2.1: Different values of impurities which are always used for the APPJ inverstigation

2.3 Pictures and first observations

As we mentioned before, it is helpful to take some pictures of the plasma plumes in order to compare them. The pictures are taken with a SONY© DSC-R1 camera. In order to magnify more the interesting area we also use a 75 mm focal lens between the jet and the camera. The gas flow is set at 1 slpm and the voltage signal at 300 mV peak-to-peak at the output of the generator. The power which is dissipated within the plasma is not known for this measurements but it has to not change to much.

2.3.1 Argon and Helium plasma

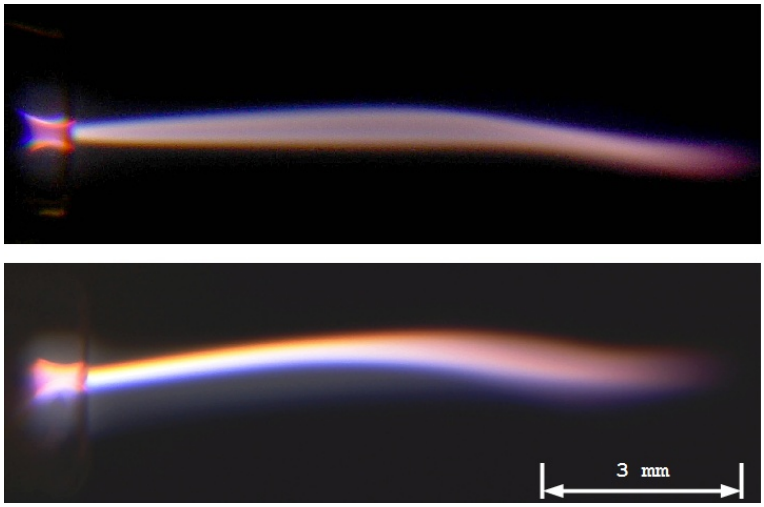

Figure 2.1: Pictures of a Argon APPJ, different exposure times.

We can see on figure 2.1 two pictures of a pure Argon APPJ[1]. The first one has an exposure time of 1/60 s while the second one is exposed 1/30 s. On both of them we can see a kind of filamentary discharge. According to [8], it is possible to say that Argon gas causes a discharge which is confined and can have a filamentary behavior. The color of the discharge is between orange and brown which may mean that the emitting spectrum is closer to the red instead of the blue part. But we will look into this in the next chapter. The length of the plume is around 11 mm. The tip of the plume seems to be more diffuse that the other end but it might due to the gas flow which could be less laminar. The discharge seems to be formed by two filaments. We can suppose this because the

[1] Actually the plasma is not a pure Argon plasma because of the air. But in our case, it means that the gas which is used in the gas flow is pure. There are no impurities added.

middle of the jet is darker than the two edges. Moreover, the discharge is not very stable in this conditions as the second half of the plume is fluctuating.

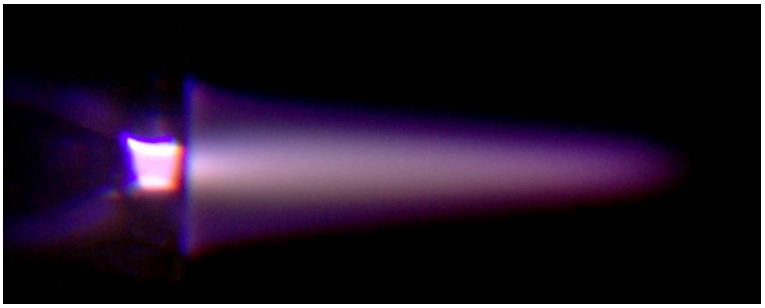

Figure 2.2: Picture of a Helium APPJ, 4.6 mm long.

Figure 2.2 is a picture of a pure Helium APPJ which is taken at an 1/20 s exposure time. The jet looks different than the Argon plasma; it is shorter, the intensity is less bright and the shape is completely different. The jet is more diffuse whereas the Argon jet is confined. Roughly we can see two parts inside. The centre which is brighter and the edge which is darker and purple. Both are separated by a small dark area. The Helium jet is completely symmetric whereas the Argon is not. It is also stable.

2.3.2 Argon with admixtures of N_2 and O_2

(a) Argon plasma jet with 0.7% of N_2, 9.4 cm long.

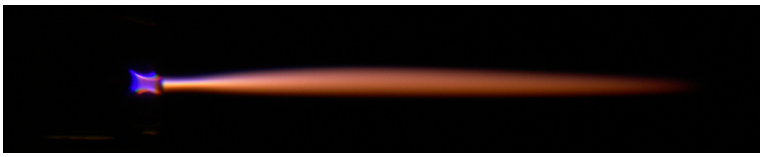

(b) Argon plasma jet with 1.3% of N_2, 8.1 cm long.

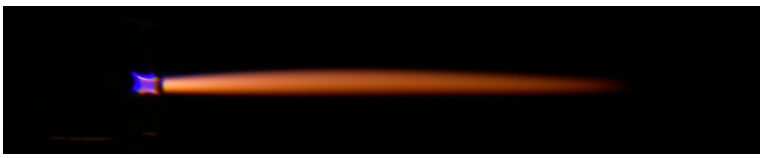

(c) Argon plasma jet with 2.5% of N_2, 7.4 cm long.

Figure 2.3: Some pictures of an Argon APPJ with different concentration of N_2; the exposure time is 1/60 s.

The figure 2.3 is a group of three pictures of an Argon APPJ with a few percent of N_2; in this case, Nitrogen is chosen as impurity. Now, we can compare them with the pure Argon pictures: from this observation we can see that with only 0.7% of Nitrogen inside the gas flow, the plume is smaller and more red. There is only one filament

at the beginning of the jet.
For increasing concentrations, the length is decreasing and the emission is redder. The part of the plasma which is very close to the end of the tube seems to be constricted whereas a few millimeters away the plasma is diffuse. This first area might be more confined according to the previous pictures and the fact of it seems to disappear as the N_2 concentration increases. Moreover, the jet is now symmetrical in length. The last picture which is taken for a gas mixture with 2.5% of Nitrogen confirm all the facts that we noticed before. That is to say the plume is shorter when there are more impurities as well as the color is redder. Finally, the filamentary area of the plasma seems to disappeared. The jet is still symmetrical and diffuse. We can add that the Argon plasma is more stable with adding Nitrogen.

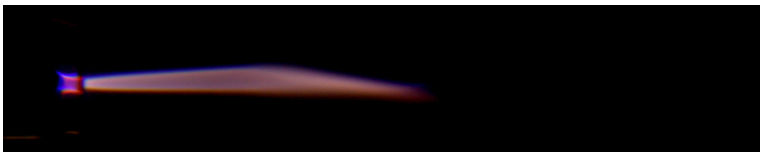

(a) Argon plasma jet with 0.7% of O_2, 5.3 cm long.

(b) Argon plasma jet with 1.3% of O_2, 3.4 cm long.

(c) Argon plasma jet with 1.6% of O_2, 2.2 cm long.

Figure 2.4: Pictures of an Argon APPJ with different concentration of O_2; the exposure time is 1/60 s.

As a next step the effect of O_2 added to the gas flow is investigated. We can see that the length of the plume is half of the pure Argon jet when only 0.7% of O_2 is added inside. This fact might mean that the plasma is more diffuse in contrast with the confined discharge that we can observe in the pure Argon case. The shape of the jet is roughly the same and is not symmetrical. Now when the concentration of O_2 is doubled. The plasma is smaller, whiter and starts to be diffuse. It is also perfectly symmetrical. The comparison with a pure Argon jet is really interesting because everything seems to be different. There is no filament as well, and the diffusion process is more present. It could be because the Oxygen atoms quench more than Nitrogen by this way, the electron density decreases significantly due to the electro negativity of Oxygen atoms. Which has to be checked further. When the O_2 concentration is increased, we can see that the jet becomes smaller. The color is also different and changes from the orange to the white. This means that the emission spectrum is set with lots of lines which are in the whole visible spectrum and maybe more; we can assume this because of the white light which is due to the sum of lots of different colors from the visible spectrum. This point will be investigated in the chapter 3. To conclude briefly on the influence of O_2 we can say that it changes the macroscopic features of the Argon plasma.

2.3.3 Helium with impurities N_2 and O_2

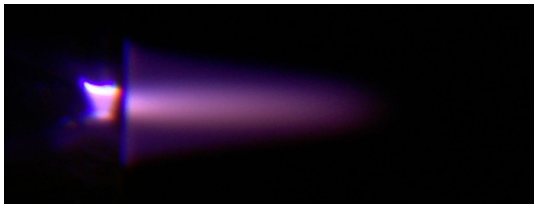

(a) Helium plasma jet with 0.7% of N_2, 4.1 cm long.

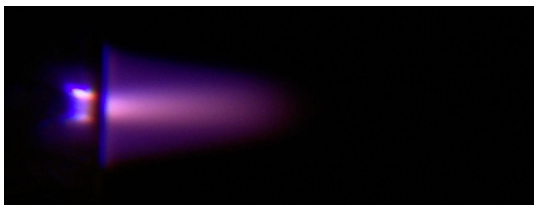

(b) Helium plasma jet with 1.3% of N_2, 3.1 cm long.

(c) Helium plasma jet with 2.5% of N_2, 2.3 cm long.

Figure 2.5: Some pictures of an Helium APPJ with different concentration of N_2; the exposure time is 1/20 s.

The impurities are also mixed with Helium. For a low ratio of N_2 in the background gas flow, there is no change if it is compared with a pure Helium plasma jet. The slight change is the length. The plasma is still diffuse and the Nitrogen doesn't seem to disrupt the He plasma. The main macroscopic factor which is changed is the size of the jet: the tip of the jet is less sharp when the ratio of impurities grows and the plasma seems to be thicker on the edges. It is possible to assume that due to the color saturation if we compare the figure 2.5a with the figure 2.5b. It is the same if the comparison is done between figure 2.5b and figure 2.5c. By this fact, the hypothesis of a more important quenching can be assumed because of the shorter length of the plume and also because of the radiation which come from the edges of the jet. The Nitrogen might enhance the quenching and thus create more diffusion in the jet. These entire hypotheses will be investigated and discussed in the next chapters of this report.

The same experiment was done with adding Oxygen. Figure 2.6 is a group of three pictures which show the jet for different concentration of impurities. It seems there adding Oxygen induces lots of changes like the optical appearance and the length of the jet. The plume is smaller when the amount of Oxygen atoms rises up to 1.3% and the intensity of the radiation seems to be lower for the same exposure time. This probably means that some species are lost due the diffusion. If we compare the color of the jet on the figure 2.6a and the figure 2.6b seems to be similar. The main color is purple with a brighter part in the centre of the jet. If the concentration of impurities is increased to 1.9%, we can see more changes. The length is decreasing as we noticed before but the color is now white. It is not possible to have a judgment about the brightness because of the different exposure. The white color means that the emission spectrum changed. The diffusion also seems to be more present in this case and that may explain why the plasma is so small but it is not sure that it is the only reason. In addition, it was not possible

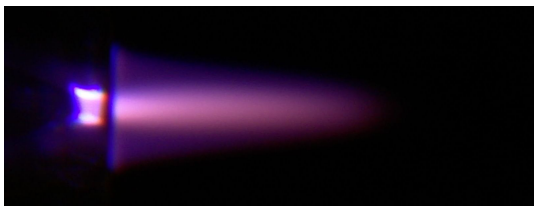

(a) Helium plasma jet with 0.7% of O_2, 3.0 cm long.

(b) Helium plasma jet with 1.3% of O_2, 2.1 cm long.

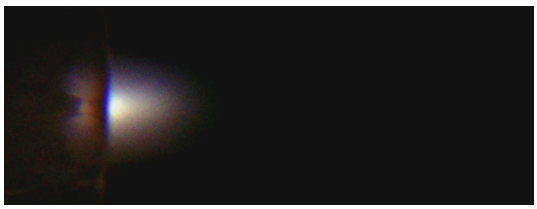

(c) Helium plasma jet with 1.9% of O_2, 1.5 cm long.

Figure 2.6: Pictures of an Helium APPJ with different concentration of O_2; the exposure time is 1/20 s for the first and 1/13 s for the last one.

to take a picture with an O_2 ratio of 2.5% because the plasma size was too small. The last-mentioned was only present around the needle electrode and inside the tip of the tube.

To conclude about the role of N_2 and O_2 it is safe to say that all the macroscopic characteristics are affected; the length, the color of the jet, the shape and the intensity. Roughly, these experiments show that O_2 induces more change in length of the plasma plume than N_2 as well for Argon and Helium. As a result, we are sure that because of the macroscopic changes there are some chemical changes too and this is exactly what it is investigated here. To look into these pictures helps to see roughly what is happening but it is obviously not accurate enough to know exactly the physical and chemical mechanisms.

2.4 Length variations for different gas mixtures

Figure 2.7 shows four series of measurements which refer to different setups. The Argon - Nitrogen gas mixture produces a longer plasma jet than the others. In this case, we can see that the length is quite stable even with 2.5% of impurities if we consider the errors of the measurement. About the error, note that for the Argon plasma, the measured length is different. This is due to the instabilities of the last-mentioned especially due to the most contracted. It is important to keep in mind that when N_2 is mixed, the jet becomes more and more stable which reduces the error. For instance, the length of the pure Helium plasma is roughly the same because of the stability of this one. When Oxygen is added inside the Argon flow we can see that the length decreases much faster than with Nitrogen. The Oxygen atoms have a big influence on it because even with 0.7% of O_2, the length of the

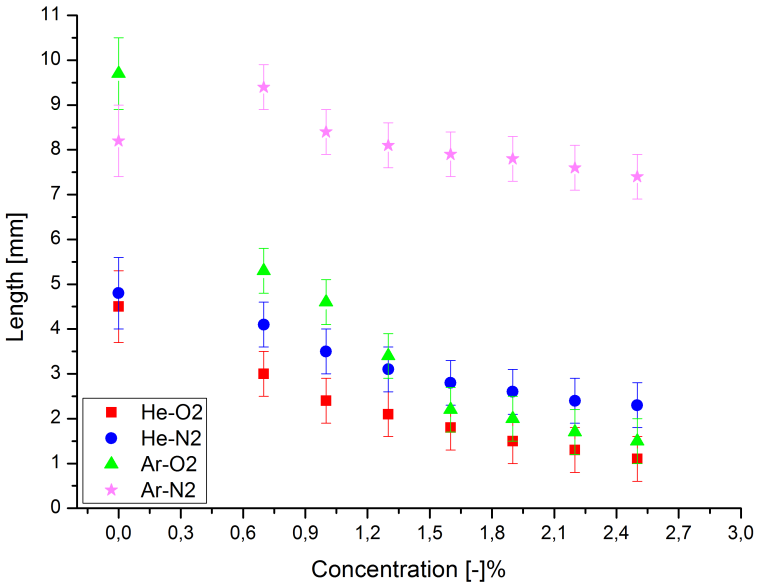

Figure 2.7: Graph of the lenghs for diffrent plasma jets.

plume is almost a factor two smaller. The fast decreasing due to O_2 is also visible on the Helium case. This fact is probably due to the quenching which is more important with Oxygen mixture. We saw on the pictures before that the plasma is also more diffuse and this may be a consequence of the diffusion of the species. The length of the plasmas with Oxygen inside seem to drop down more that with Nitrogen mixtures. As it is shown on the same graph, the plasma jet created with Helium and Nitrogen is longer than with Oxygen even in the case of Helium plasma compared to an Argon Oxygen plasma. Moreover, if we look at the relative variations of the lengths for the Argon Nitrogen mixture and the Helium Nitrogen mixture, there are roughly 2 cm of difference between the longest and the smallest length. This is not the case when Oxygen is put with Argon or Helium. The length does not differ to much that showing the physical mechanism are not the same between Nitrogen and Oxygen.
In order to investigate further the phenomena and the changes which are in the plasma, we look into the emission spectrum of the plasma jet.

Chapter 3

Optical Spectroscopy for Diagnostics: wide investigations

The spectroscopy is a very narrow field of the atomic-physics. However, it is absolutely essential to use this kind of techniques if you want to investigate more the plasma. The pictures that we took before do not give a lot of information that is why we use the spectroscopy in order to look into the spectra of the different jets. It is also because the spectroscopy is not an intrusive method that it is really useful for plasma diagnostics.

3.1 Emission spectroscopy: brief overview

The purpose of this section is to introduce some basic knowledge about the emission spectroscopy[1][14]. A simple and quick definition of the spectroscopy could be the investigation of the light by the electromagnetism concept of the wavelength. It is easily understandable because all the Human being is using some spectroscopy skills when we are able to make out different colors. The visible spectrum is from 380 to 780 nm but it is too narrow for a good diagnostic and usually people look into a wider range, typically from 200 to 1000 nm. For wavelength below 200 nm you need specific conditions because the ultraviolet radiation is absorbed by the air and the quartz too. For wavelength larger than 1000 nm it is also more difficult due to the thermal emission (black body) which can add too much noise in the signal. We also need specific detectors and IR optics. For the glow discharge the emitted light is the consequence of the excitation states. As in plasma, high energetic electrons exits the collisions between these electrons and atoms, ions and molecules are going to excite electrons which are bounded in the outer shell of the atom. The atoms get more energy and some electrons go to a higher energy level. But this state is not stable for the electrons and they try to lose it. Usually, the energy loss is spontaneous and the electrons drop to a lower energy level to emit a photon. These photons are at the origin of the light of the glow discharge. Figure3.1 shows a simple mechanism of the spontaneous emission. The ground state which is the most stable for the molecules is usually labeled X and the first excited energy level is labeled A. The energy of the photon is known by the relation 3.1 with E_i the low energy level, E_j the high energy level, h is the Planck constant, c is the light speed, λ

[1] We only refer to the emission spectroscopy and not to the absorption spectroscopy because we do not use it in this report.

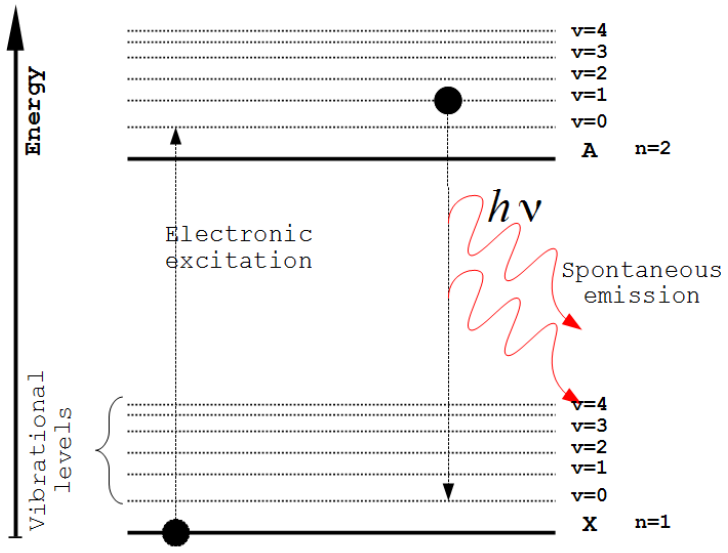

Figure 3.1: Diagram of the spontaneous emission and the electronic structure of a virtual molecule.

is the wavelength and ν the frequency.

$$\Delta E = E_j - E_i = \frac{h \cdot c}{\lambda} = h \cdot \nu \tag{3.1}$$

It is also interesting to have a look at the line emission coefficient ε_{ij} which is given by the equation 3.2 with A_{ij} the Einstein emission coefficient which is a emission probability factor, $n(p)$ is the particle density in the same state and λ_0 the central wavelength of the emission line.

$$\varepsilon_{ij} = n(p) \cdot A_{ij} \cdot \frac{h \cdot c}{4\pi \cdot \lambda_0} = \int_{line} \varepsilon_\lambda d\lambda \tag{3.2}$$

We can see that the particle density is $\varepsilon \propto n(p)$ which is useful in order to know some important plasma parameters because $n(p) = f(T_e, T_n, n_e, n_n, \dots)$ with T_e, T_n the electron and neutral temperature and n_e, n_n the electron and neutral density. It depends on the experimental conditions and it is still not possible to know these parameters because of their dependence with other phenomena.
About the emission line that we can have in the spectrum, all of those are not always transition lines. The spectrometry is based on quantum mechanics and it is possible to use quantum numbers to identify the emission lines. For the diatomic molecules each transition state with the same quantum number n is divided in vibrational levels. Each vibrational level with the same quantum number ν is also divided in rotational level which are identified by the quantum number J. Because of these subdivisions of levels, we understand that the order of magnitude of the energy is different and the rotational energy levels are smaller than the vibrational ones. The energy between the first excited level $n = 2$ and the ground state $n = 1$ is called resonant transition and its energy is usually one of the highest. Thus its wavelength is usually close to the ultraviolet. As the electronic structure is complex it is impossible to look at the transitional lines and the rotational lines with the same spectrometer. As a consequence, it is important to know what you want to investigate in order to use the appropriate device.

3.2 Setup of the diagnostic

The investigation of the jets are done with two different spectrometers from Ocean Optics©. The aim of these measurements is to look at a large spectrum in order to see some transition lines. With these lines it is possible to know what is happening in the plasma, for instance the creation of reactive species such as OH, NO,...
About the setup and the conditions of the experiment you can refer to the figure 3.2 which is a simple sketch and shows the main devices that we used. The plasma jet is supplied by the same signal generator which is coupled with the amplifier. The output voltage is fixed at 300 mV at the output of the signal generator. The gas flow is fixed at 1 slpm and is either Argon or Helium. Obviously, Oxygen and Nitrogen are mixed inside with different concentration but not at the same time. The wavelength range that we want to observe is really wide because it starts roughly between 200 nm to 950 nm.

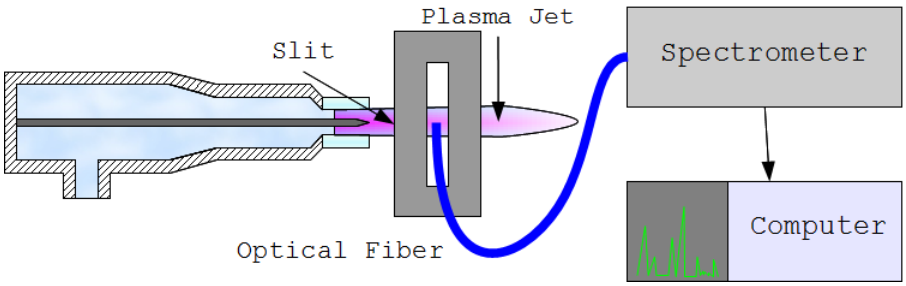

Figure 3.2: Scheme of the setup for the spectroscopy diagnostics.

To get a spectrum with a big range of seven hundred nanometers, we must use several spectrometers. Thus, the measurements are done with two Ocean Optics© spectrometers HR 2000 and HR 4000. The characteristics of each of them are given in the table 3.1. In order to take the light from the jet to the input of the spectrometer, the optical fiber QP 400-2-UV and QP 600-2-UV from Ocean Optics© are used. Then, at the tip of the fiber, a slit was added in order to control the investigated area of the plume. The width of the slit is adjustable and we check its influence on the spectra. The result is just seen a decrease of the intensity. Thus, the slit width is fixed at 1.0 mm.

Model	HR 2000	HR 4000
Range	177 - 622 nm	500 - 947 nm
Grating	600 L/mm	600 L/mm
Blazed	400 nm	1 μm
resolution	230pm	230pm
Slit	50 μm	5 μm
Detector	Sony© ILX 511-UV2	TCD© 1304AP

Table 3.1: Characteristics of the spectrometers Ocean Optics©.

The software of Ocean Optics© is used for data acquisition. All the spectra are the results of five spectra which are averaged in order to reduce the measurement error. The exposure time is adjusted according to the intensity of the radiation and to use the full intensity range of the spectrometer. But to compare all the spectra, they are normalized in intensity during the post-processing.

3.3 Light emission of Argon and Helium plasma jets: first spectra

3.3.1 Argon plasma jet spectra

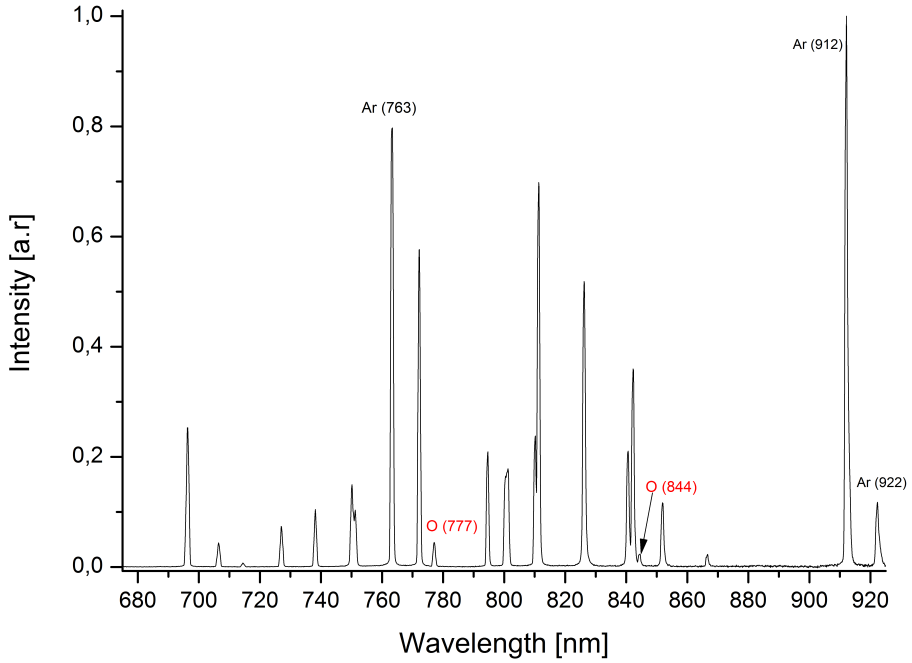

Figure 3.3: Spectrum of the Argon APPJ from 650 to 930 nm.

Figure 3.3 is the spectrum of the pure Argon APPJ from 650 to 930 nm. This part of the plasma radiations is from the red spectrum to the near-infrared spectrum. We can see many lines which are the consequences of the electron transitions between a high energy level to a lower energy level. All of the lines comes from the Argon electronic structure which is exited by all the species within the plasma except at 777 and 844 nm. The highest Argon peak is at 912 nm. The 777 and 844 nm are the transitions from the atomic Oxygen. The relative intensity of this peak is only 5% of the highest Argon peak but the presence of it shows that there is creation of atomic Oxygen. The amount of atomic Oxygen which is created seems to be small if we look at the intensity of its peak. Actually, it is difficult to answer this question because the Argon lines intensities are very high compared to the averaged emission. Moreover, according to the previous chapter, the Argon jet is quite bright and it is due to the Argon lines. The Oxygen excitation may due to the Argon plasma and the Oxygen source is the air from the room. So, there are some exchanges between the plasma and the surrounding which is a good point. The production of atomic Oxygen will be investigated more in the section 3.4.2. Except the Argon and Oxygen line, there is no other line in this spectrum. The main reason is because this range of wavelength corresponds to the low transition energies which mean that is difficult to excite other species. The transition gap for exiting N_2 or to create OH, NO, etc. is much higher than the energies which are evaluable in this range.

If we look into the spectrum from 250 to 600 nm on figure 3.4, we can notice interesting things. To make a link with the previous spectrum on figure 3.3, we can say that there is no emission line in the range 450 to 690 nm. The resolution is not able to give more details from this range. If we look at the spectrum, we can see tree high peaks from N_2 transitions. There are only two lines from Argon at 416 and 420 nm respectively. These lines are not very intense and are just at the limit of the visible spectrum. The fourth highest peaks are in the ultraviolet A which is interesting because of the energy of these part of the spectrum. The farthest peak in this spectrum which

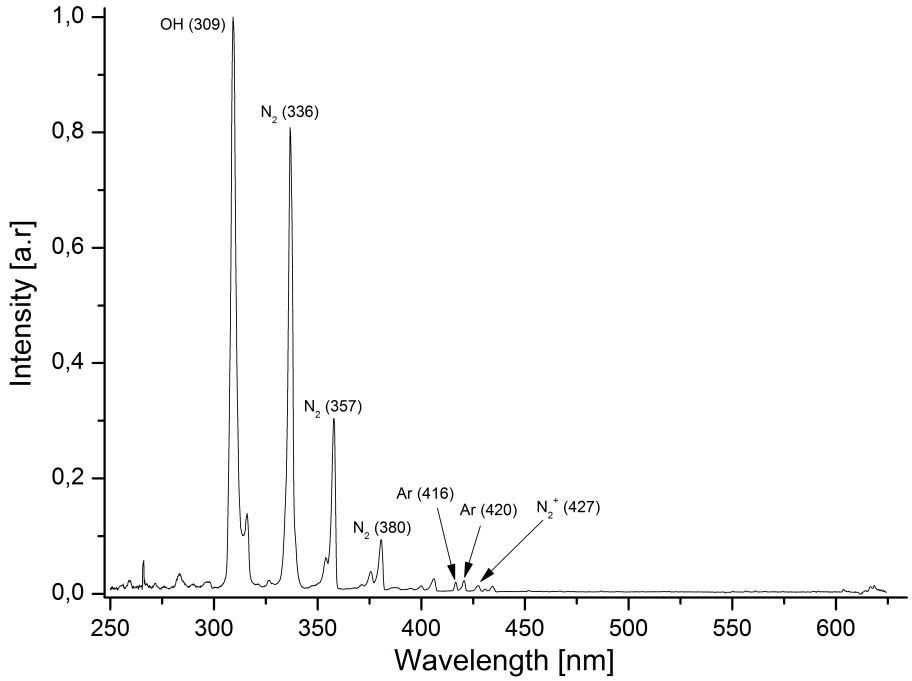

Figure 3.4: Spectrum of the Argon APPJ from 250 to 600 nm.

is also at the highest energy is the transition of OH at 309 nm. Its intensity is the highest peak intensity which means that the production of OH is significant. This element is useful to get an estimation of the gas temperature. As its intensity is high, the spectrum of it can be accurate and help to reduce the error of measurement. This species is also interesting to produce because it is a reactive species which means that it is able to react easily and quickly with a lot of molecules. It is also possible to see a N_2^+ peak at 427 nm. Its intensity is a few percents of the maximum intensity.

3.3.2 Helium plasma jet spectra

Figure 3.5 is a spectrum of a Helium APPJ. The investigated range is from 550 to 900 nm. As the figure 3.3 shows, it represents the transition lines for the low radiation energy. Because of its electronic structure the Helium atom has less visible transition lines than Argon but its first ionization energy is higher than for Argon. Helium ionization potential is 24.59 eV and Argon is 15.76 eV. We can see that the highest peak of Helium at 706 nm. It is also possible to see the H_α line with an intensity of 42 %. There are also some bands due to the vibrational energies of N_2 from the first positive system. As in the Argon case, there is also production and excitation of atomic Oxygen with a Helium APPJ. Atomic Oxygen has its peaks at 777 and 844 nm. The intensity of the peak 777 nm is the highest which means that atomic Oxygen is exciting really well by Helium. The reaction 3.3 is probably the more often reaction which can happen in order to excite atomic Oxygen. It needs around 16 eV to dissociate and excite Oxygen.

$$\mathrm{He}^* + \mathrm{O}_2 \longrightarrow \mathrm{He} + \mathrm{O} + \mathrm{O}^* \tag{3.3}$$

Nonetheless it is not possible to know by those spectra if the atomic Oxygen production is higher with Helium than Argon because of the normalization. If we look for the intensities of the He 706 nm line and Ar 763 nm line on

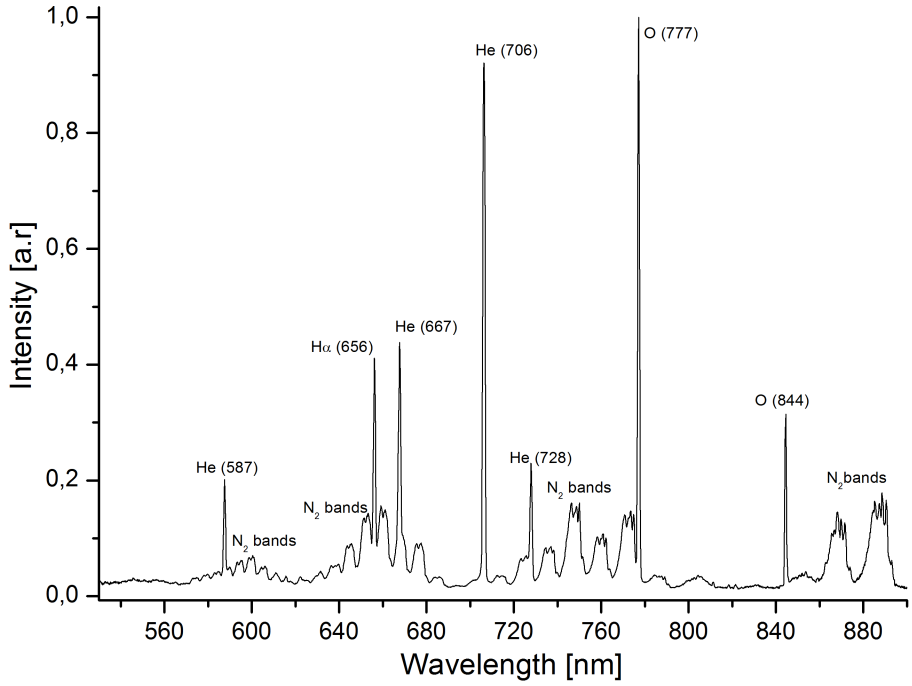

Figure 3.5: Spectrum of the Helium APPJ from 520 to 920 nm.

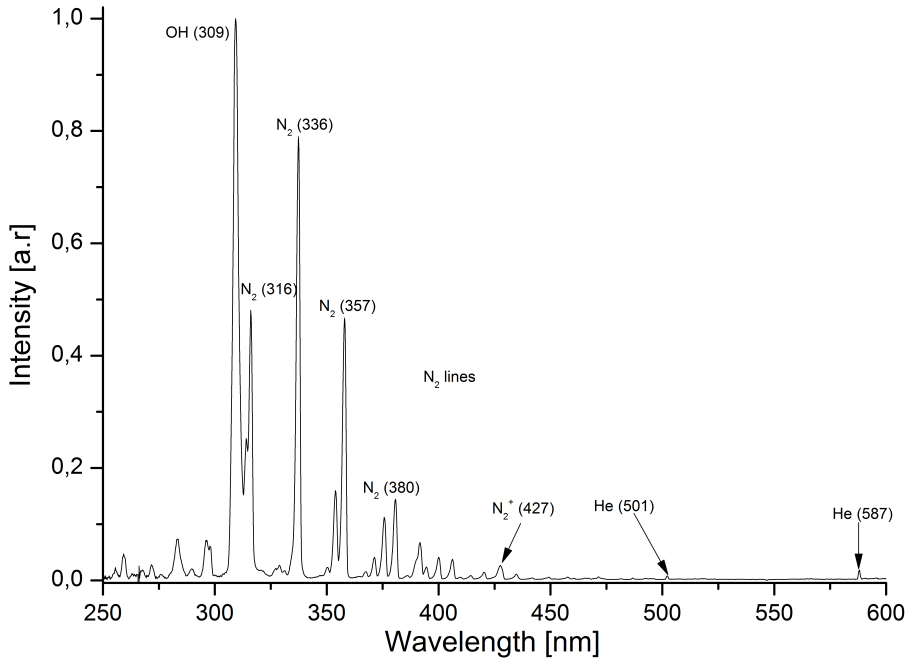

Figure 3.6: Spectrum of the Helium APPJ from 250 to 600 nm

NIST website[2], we could deduce which plasma produces the most of atomic Oxygen. But the intensities on NIST website are relative intensities and we did not calibrate the absolute amplitude sensibility of the monochromator.

Figure 3.6 shows the spectrum of He in the range 250 to 600 nm. Many of peaks are visible and most of them come from the N_2 radiations. The N_2^+ is visible at 427 nm such as in the Argon case. The N_2 lines are thinner than for the lower energies on the previous graph. As N_2 needs a high energy to be exited, it is normal that the radiations are more significant close to the UV. We can also see the OH peak at 309 nm which is the highest as the Argon case. All the radiations from N_2 and OH contribute to the UV emission of the jet. This characteristic is interesting because it is a high available energy. Helium seems to excite more the N_2 molecules instead of Argon because the number of N_2 lines is higher in the helium spectrum. It is probably due to the energy level which is needed to pre-ionize Helium atoms because N_2 needs high energies be pre-ionized. Moreover, most of the emissions of N_2 molecules is between 180 and 380 nm.
It is interesting to investigate more the influence of the impurities. All the species emissions that we can see on the previous spectra of Argon and Helium come from the surrounded impurities. What is happened if N_2 or O_2 are mixed with the Argon or Helium gas flow before to be ionized? We did these experiments and analyze the emissions of the different jets.

3.4 Focus on the influences of the impurities

3.4.1 Influence of Nitrogen on Argon APPJ emission

Adding Nitrogen in the Argon gas flow induces some changes in the plasma. First of all, it seems that Nitrogen helps to get a more stable discharge than pure Argon. We have noticed this in the previous chapter, section 2.3.2. The optical appearance is more red with N_2.

Figures 3.7 and 3.8 show two spectra of a pure Argon APPJ and a Ar-N_2 mixture for two different positions. This wide spectroscopic investigation confirms that the emission in the orange and red range[3] is higher when Ar is mixed with N_2. If there is no big change just at the tip of the needle, seven millimeters away we can see that the Argon lines are covered by the vibrational emission lines of N_2. The intensities of these lines are also higher than around the needle. If we look at the spectrum on figure 3.8, we can see several peaks in the near UV range, such as OH and some N_2 bands. The emission in the visible spectrum from 400 to 600 nm is weak at either at 0 mm or at 7 mm for pure Argon APPJ. It is weak too when Argon is mixed with N_2 at 0 mm but it increases a lot at 7 mm even if it is not significant compared to the other part of the spectrum. We can see that the intensity of OH is also going down but there is no big change from 200 to 480 nm range. The biggest variation comes from 480 to 800 nm for the spectrum at 7 mm away.

In this range we notice that the Nitrogen molecules are highly exited especially after several millimeters from the end of the tube. The Nitrogen emissions are well known that is why we can assume that the big peaks from 575 to 800nm are due to the N_2 excitations. It is from the state $B^3\Pi_g$ to $A^3\Sigma_u^+$ which represents the First Positive System [15]. Figure 3.9 shows these different Nitrogen energy levels. These transition lines have a low energy level that is why there are closer to the red or even infrared spectrum than the ultraviolet spectrum. Which is interesting is that the $A^3\Sigma_u^+$ of N_2 is a metastable state. It means that the life time of this energy level is a few magnitudes longer than the others. As the intensity of the lines which provide the state $A^3\Sigma_u^+$ are high and large we can deduce that the Nitrogen population in this state is also large. The quenching with the electrons but with

[2] http://physics.nist.gov/PhysRefData/ASD/lines_form.html

[3] It is agreed that the orange spectrometric range is around from 590 to 625 nm and the red spectrometric range is from 625 to 780 nm.

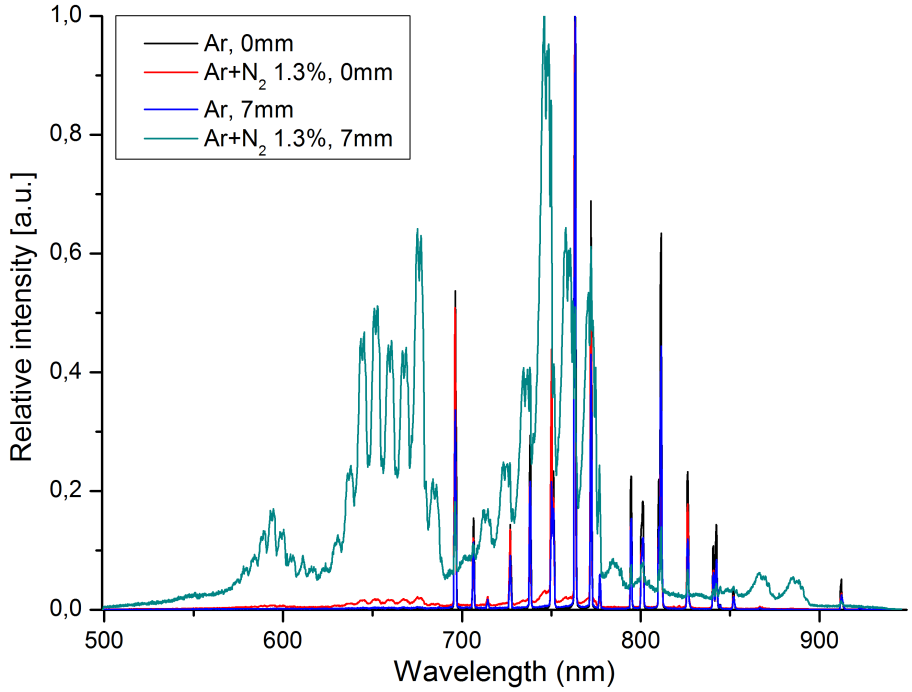

Figure 3.7: Spectrum of the Argon APPJs from 500 to 930 nm.

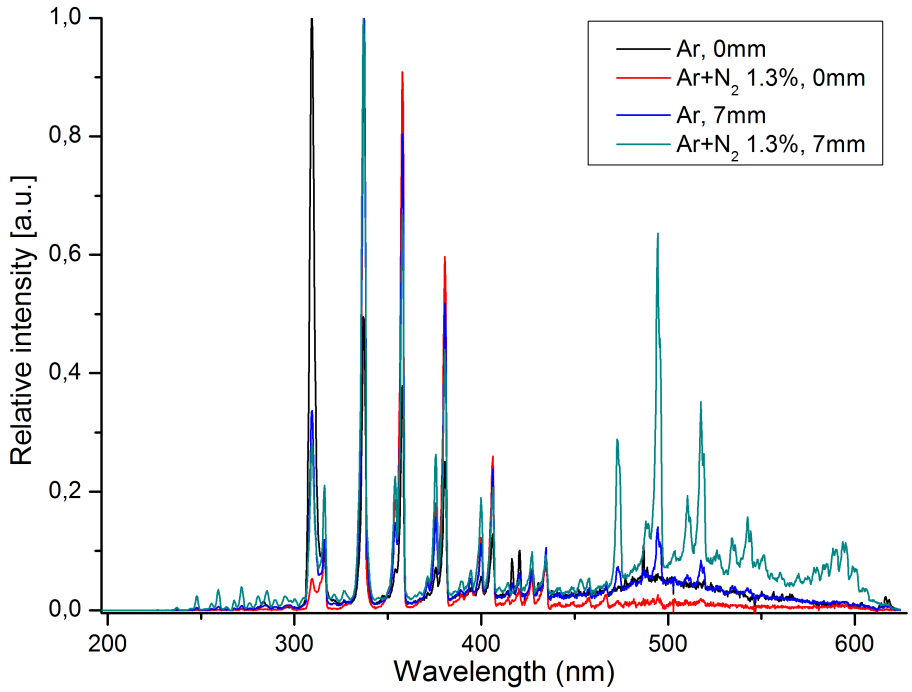

Figure 3.8: Spectrum of the Argon APPJs from 200 to 630 nm.

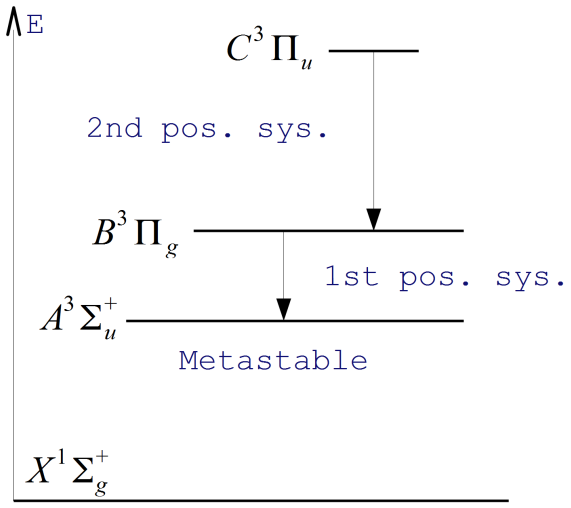

Figure 3.9: Simple schematic structure of the Nitrogen energy levels.

another atom of Argon in the same state is possible. The collision between two Nitrogen metastables has a good probability to happen.

$$\mathrm{N}_2^*\left(\mathrm{A}^3\Sigma_\mathrm{u}^+\right) + \mathrm{N}_2^*\left(\mathrm{A}^3\Sigma_\mathrm{u}^+\right) \longrightarrow \mathrm{N}_2^*\left(\mathrm{X}^1\Sigma_\mathrm{g}^+\right) + \mathrm{N}_2^*\left(\mathrm{C}^3\Pi_\mathrm{u}\right) \pm \Delta\mathrm{E} \tag{3.4}$$

The reaction 3.4 illustrate the mechanism of the energy transfer. This reaction is called *Energy-Pooling Collision* according to Bicchi [16]. The variation of the energy ΔE is the energy balance of the process. It is also the main factor which determines the feasibility of the reaction. The $C^3\Pi_u$ energy level is a higher level and will have a radiative transition to go into the $B^3\Pi_g$ state. The mechanism is cyclical but because of the probability of collisions and of the waste of energy, there is less and less emissions as far the species travel into the plasma jet. We can consider also two other reactions with the equations 3.5 and 3.6. For the first one, Argon metastable has a collision with a ground state Nitrogen molecule. Then, some electrons which have enough energy can also excite Nitrogen from the ground state.

$$\mathrm{Ar}^*\left({}^3\mathrm{P}_{2,0}\right) + \mathrm{N}_2\left(\mathrm{X}\right) \longrightarrow \mathrm{N}_2^*\left(\mathrm{C}^3\Pi_\mathrm{u}\right) + \mathrm{Ar}\left(\mathrm{X}\right) \tag{3.5}$$

$$\mathrm{e} + \mathrm{N}_2\left(\mathrm{X}\right) \longrightarrow \mathrm{N}_2^*\left(\mathrm{C}^3\Pi_\mathrm{u}\right) + \mathrm{e} \tag{3.6}$$

To make a link with the spectrum on figure 3.7 we can see that the red color of the jet is due to the mechanism of N_2.

The figure 3.10 shows the area calculation of different spectra for the pure Argon APPJ and a Ar-1.3% N_2 at different positions from the tip of the needle. It is clear that the area of the orange and red range is the biggest. We can see that the emission from 200 to 630 nm is quite constant especially for pure Argon APPJ. From 4 mm to 10 mm we can see that the emission from N_2 is high which confirm what we said in the section 2.3.2. The emission of N_2 is also higher because of its concentration. Further from the needle the plasma is and more air is mixed with the plasma which enhances the quenching and increases the excitation process for N_2.

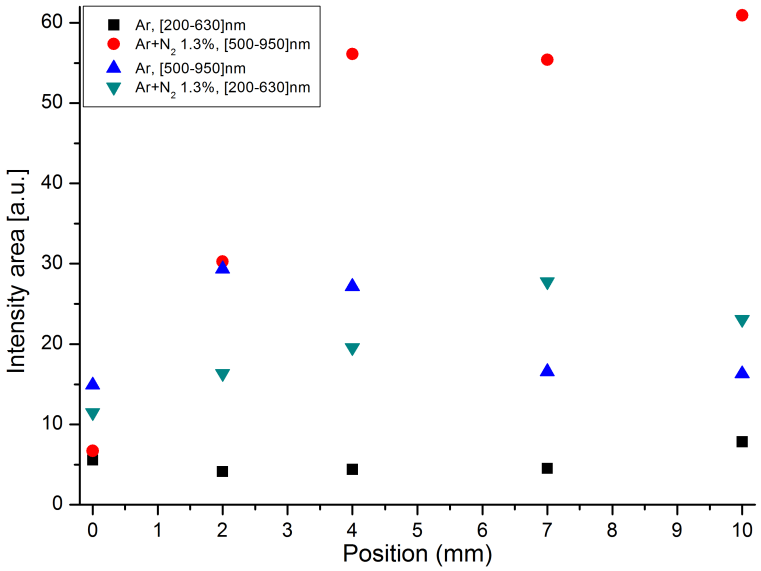

Figure 3.10: Relative radiation sum of the different spectra of figures 3.7 and 3.8

3.4.2 Oxygen excitation in Argon plasma

We know that the Argon APPJ properties can change if Oxygen is added. By spectroscopy measurements it is possible to look at the emissions of the jet and understand what is happening in the plasma. Figure 3.11 shows

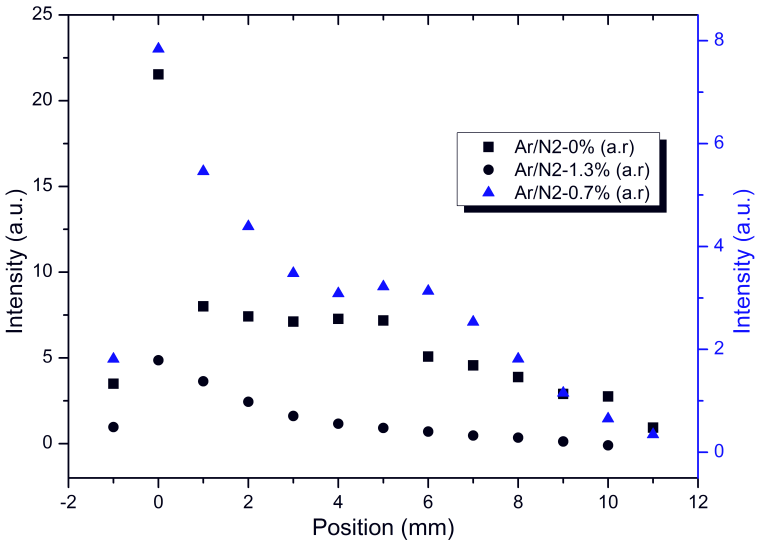

Figure 3.11: Relative intensity of the Oxygen line, 777 nm along the jets.

three intensity curves versus the position in the plasma jet. The origin is the tip of the needle electrode. The negative position means that the light is from the plasma part which is around the needle. The intensity for this position is subdued due to the absorption of the glass tube. There is no reason to have the same physical reactions along all the jet. The emissions of the transition energies are necessarily not identical along the plume that is why we investigate the jet for different position. To compare the influences, three different gas mixtures are used such as pure Argon which is the reference, and Argon with 0.7% and 1.3% of N_2. We can see that the intensity of the Oxygen line is smaller for a high concentration of N_2. But a few percents of N_2 seem to get a higher intensity of the Oxygen line. That means the amount of excited atomic Oxygen is higher too.

If we compare a pure Argon plasma jet with Argon and 0.7% of Nitrogen we can say that the shape of the curve

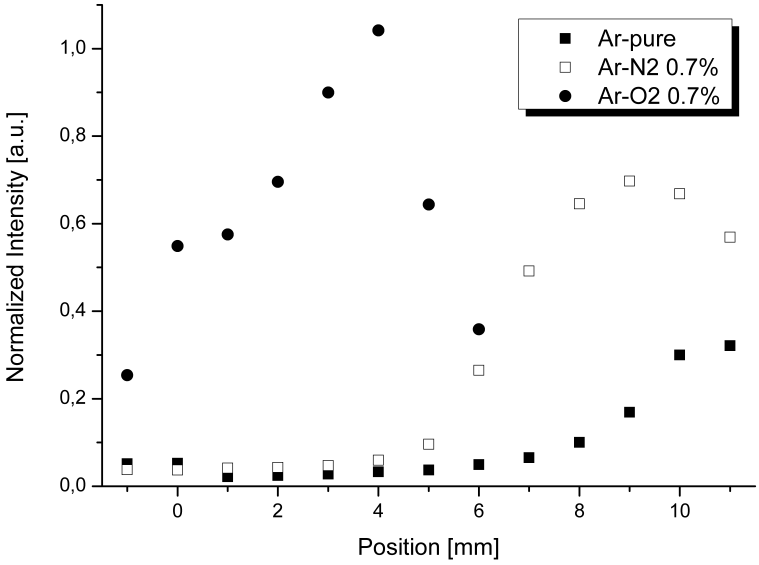

Figure 3.12: Relative intensity of the Oxygen line, 777 nm along the jet for different gas mixture.

is roughly the same with a plateau from 3 to 6 mm in front of the tip of the needle. The Oxygen emission is constant in this range which means that the excitation of the atomic Oxygen is contant too. After 6 mm the Oxygen emission decreases which means that the amount of excited atomic Oxygen decreases too. It decreases faster for the cases where N_2 is mixed with Argon. It could be due to the quenching. Along the first millimeters N_2 can help to dissociate molecular Oxygen because of the quenching and the electron density which is higher than at the end of the jet. More quenching means a high collision probability with O_2 and if the energy of the electrons is high enough, O_2 can be dissociated. Obviously, if the quenching is dominant, electrons loose too much energy and cannot excite O_2. This graph seems to show a dependency of the N_2 concentration which enhances or reduces the atomic Oxygen emission.
If we want to increase the excitation of Oxygen, it is obvious to make a test with an Argon and Oxygen mixture. In order to know the influence of the Oxygen concentration in the gas flow we have to compare a pure Argon jet with the Argon and Nitrogen mixtures which produced most of atomic Oxygen. Similarly to figure 3.11 we add 0.7% of Oxygen and Nitrogen to the Argon flow. Figure 3.12 shows three curves of the normalized intensity of Oxygen peak at 777 nm versus the position inside the jet. It is important to mention that the intensity is normalized in comparison to the highest Argon peak at 763 nm. Which the highest of the spectra. We can see that a mix of a few percents of Nitrogen with Argon produces more atomic Oxygen emission than pure Argon. This matches well with the previous figure and what we already observe. From 6 mm to 11 mm we can see that the Oxygen line increases against the Argon line. This is probably due to the Argon-Oxygen ratio. After a few millimeters the Argon is more diffuse and the ratio of Oxygen increases because of the surrounding air.
In the case of Argon mixed with Oxygen, we can see that the atomic Oxygen emission is rising linearly from -1 mm to 4 mm. At 4 mm the Oxygen emission is even higher than Argon emission which means that there is bigger production of atomic Oxygen. From 4 mm to 6 mm the relative intensity of Oxygen decreases rapidly. The Argon-Oxygen plasma is more diffuse than the pure Argon or Argon-Nitrogen plasma, so the Argon atoms which are in this area have less energy and cannot dissociate Oxygen molecules anymore.

The oxygen excitation process in this plasma can be explained by different reactions. Figure 3.13 shows the different energy level of Oxygen. If we only consider the electron influence, we know that Oxygen is a high

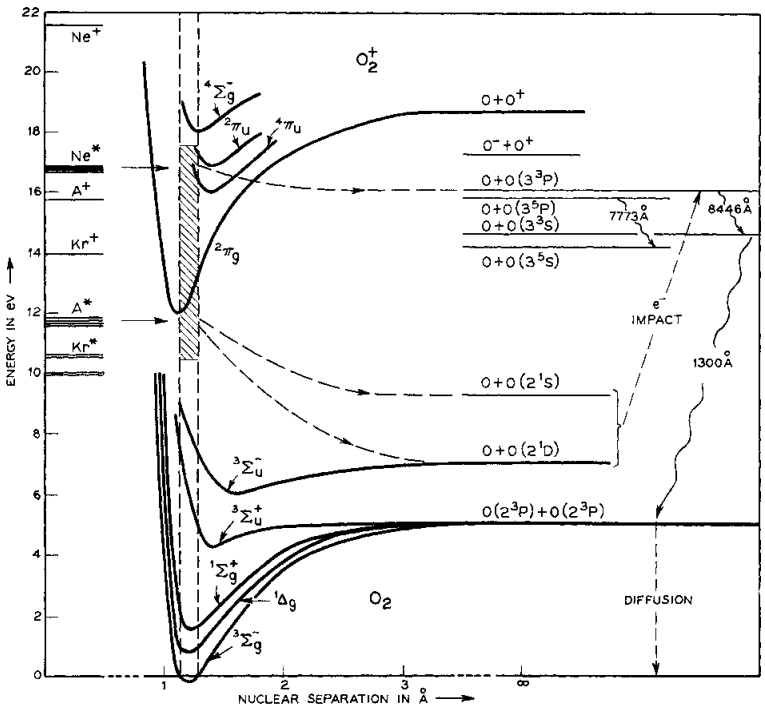

Figure 3.13: Relevant energy levels of Oxygen[5].

electronegative element with 3.44 on the Pauling scale[4]. This means that the Oxygen molecules are a good catcher of electrons. By this way, it is possible for an electron which has enough energy to break the molecular bond. This reaction is represented by the equation 3.7 [17] of the dissociative attachment.

$$e + O_2 \longrightarrow O + O^- \tag{3.7}$$

To get this reaction the electrons should have enough energy thus the higher probability get it is as close as possible to the needle and the electrons must have a bit more than 16 eV. This mechanism enables the plasma to create atomic Oxygen. But this is not the main reaction because of the needed energy and Argon is also important in this process. Close to the needle, the electric field is intense which can accelerate the electrons. By this way they must get a high energy which is enough to pre-ionized Argon atoms.
We consider also that Oxygen can be ionized according to the reactions 3.8 and 3.9. Then the Oxygen anions and cations can have a collision and excite one of them whereas the other goes to the ground state as shows the equation 3.10 with a rate of 10^{-13} m^3s^{-1}. This process has two step and we get the emission from the upper level to the lower energy level.

$$e + O_2 \longrightarrow O^- + O \tag{3.8}$$

$$e + O_2 \longrightarrow O^+ + O \tag{3.9}$$

$$O^+O^- \longrightarrow O^* + O \tag{3.10}$$

The atomic Oxygen which is still at the ground state can also be excited by an other process. According to [17, 18, 19] we know that Argon has two interesting metastables states in the same energy range as Oxygen, $^3P_2$, 11.72 eV and $^3P_0$, 11.54 eV are both metastables with a lower energy than the ionization energy of Oxygen

[4]the maximum electronegative element is the fluorine with 3.98 on the Pauling scale

which is at 13.62 eV. But, if it is not possible for them to ionize Oxygen, it is possible to dissociate molecular Oxygen according to the reaction 3.11[5] and created Oxygen metastable. Then, the metastable Oxygen can be excited by a collision with an electron, reaction 3.12.

$$\mathrm{Ar}^{*}_{\mathrm{metastable}} + \mathrm{O}_2 \longrightarrow \mathrm{O} + \mathrm{O}_{\mathrm{metastable}} + \mathrm{Ar} \tag{3.11}$$

$$\mathrm{e} + \mathrm{O}_{\mathrm{metastable}} \longrightarrow \mathrm{O}^{*} + \mathrm{e} \tag{3.12}$$

The Argon metastable can also have a collision with atomic Oxygen as shows the reaction 3.13. The rate of this reaction is around 10^{-13} $\mathrm{m^3 s^{-1}}$[18, 19] which is similar to the reaction refeq:Ox+-

$$\mathrm{Ar}^{*}_{\mathrm{metastable}} + \mathrm{O} \longrightarrow \mathrm{O}^{*} + \mathrm{Ar} \tag{3.13}$$

We do not know exactly which reactions between the equation refeq:Ox+- and refeq:Ox6 are dominate. But we can assume that the process of atomic Oxygen excitation is due to two reactions at least. The reaction 3.14 with an electron which can dissociate O_2 and excite one Oxygen atom is not credible because we need to much energy. If this reaction happens, it will be not the main process.

$$\mathrm{e} + \mathrm{O}_2 \longrightarrow \mathrm{O} + \mathrm{O}^{*} + \mathrm{e} \tag{3.14}$$

The energy needed and the different reactions explain why the amount of the atomic Oxygen line intensity decreases after a few millimeters long according to the figure 3.12. It is basically because the amount of Argon metastables decreases and the electron energy density decreases too along the plume.

3.4.3 Influence of Nitrogen and Oxygen with Helium

Some experiments are also done with a Helium APPJ and as with the Argon cases we have mixed a few percentages of Nitrogen and Oxygen. As we have already said, the Helium APPJ is more stable than the Argon plasma explaining why there is no change if we add Nitrogen or Oxygen with the Helium flow. The main visible impact is with Oxygen because the plume is smaller than before.

Figure 3.14 is a graph which contains three spectra for different conditions. The observation range is from 550 to 900 nm. We can see that the relative spectra of pure Helium and with 2.2% of Nitrogen are quite similar. We can see, as with in the Argon case, three big peaks from a few large bands of the Nitrogen first positive system. The width of these lines depends on the vibrational and rotational energies of each transition. We also notice that these bands are visible with a pure Helium APPJ. It means that the Nitrogen of the air is diffusing and mixing into the plasma to be excited. If we look at the spectrum of the Helium mixed with 2.2% of Oxygen, we can say that the Nitrogen emission is smaller than the two previous cases. Actually this spectrum is slight and simple. There are only the emission lines of Helium and atomic Oxygen at 777 nm and 844 nm. We can see of the excitation lines of the Nitrogen which show us that Nitrogen molecules are diffusing into the plasma. The production of atomic Oxygen seems to be high because the intensity of the line 777 nm is the highest of this spectrum, even higher than the Helium lines. The calculation of the integral from 550 nm to 900 nm for the Helium mixed with 2.2% of Oxygen is only 20% of the pure Helium APPJ spectrum. This fact is coherent with the pictures that we took in the section 2.3.3. The plasma is more diffuse probably because of the electronegativity of the Oxygen molecules which catch the electrons. The plasma has more waste of electrons and the excitation of the molecules is less efficient. The integral of the spectrum with Helium and Nitrogen is 50% higher than the pure Helium which

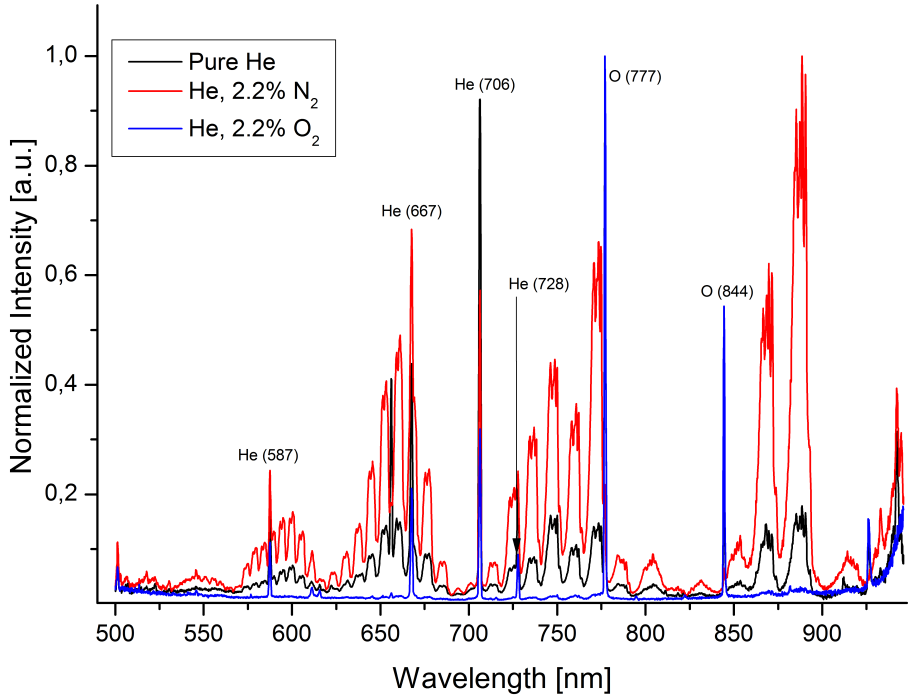

Figure 3.14: Spectra of Helium APPJ with 2.2% of Nitrogen or Oxygen from 550 to 900 nm

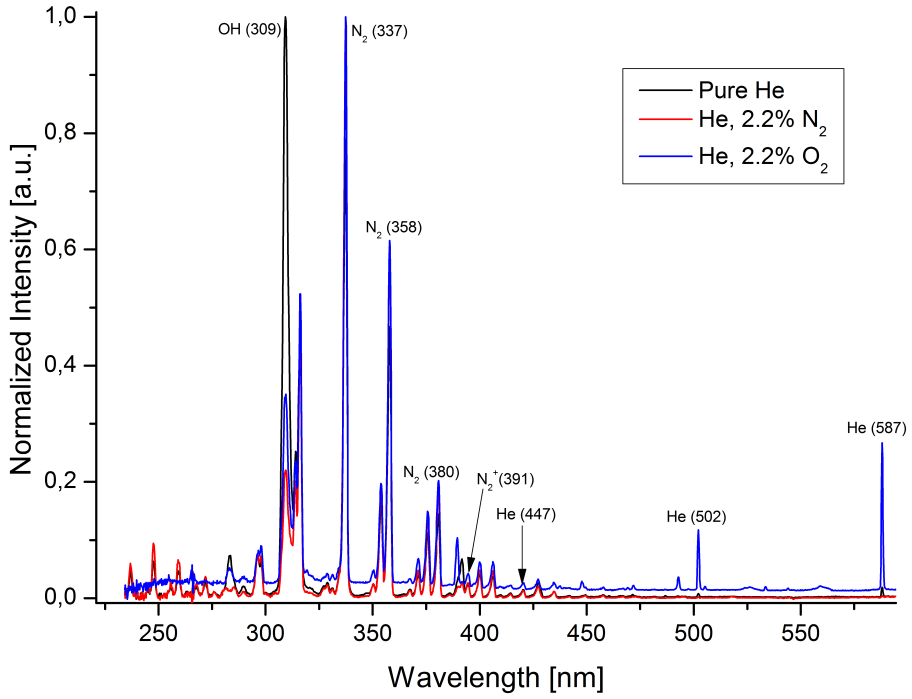

Figure 3.15: Spectra of Helium APPJ with 2.2% of Nitrogen or Oxygen from 300 to 600 nm

means that the amount of excited molecules is also higher and the electron density may be higher too. But it is just a qualitative description from the spectrum analysis.

Figure 3.15 shows three spectra for the same configuration as before from 300 to 600 nm. For two mixtures, except the one with Oxygen, it is possible to see lots of Nitrogen molecule lines. These correspond to the second positive system of the Nitrogen transitions. It is the energy from the $C^3\Pi_u$ state to the $B^3\Pi_g$ state. It is also for the pure Helium and the mixture Helium-Nitrogen that there are the most of transitions lines. The Helium peak at 502 nm is the highest of the Helium Oxygen mixture spectrum and shows that the intensity of these lines is lower for this mixture. The calculation of the spectra integrals show us that the APPJ Helium Oxygen mixture Intensity is only 7% of the pure Helium one from 300 to 600 nm. The whole intensity of the Helium Nitrogen mixture is 150% higher than pure Helium APPJ which means that the N_2 transitions are the main reactions in the plasma. Finally, there is no big change with the Argon APPJ. The Nitrogen excitation seems to be higher with Argon because of the intensity of its transitions. There is no other species which could be created with the Helium APPJ line neither NO nor O_3 and the UV emission is also lower than in the Argon case.

Chapter 4

Power investigation

One of the most important parameters in plasma physics is the power. The plasma is most of the time controlled by the power because it is easy to do with a generator and it is very sensitive compared to other parameters such as the pressure which is more difficult to use for controlling the plasma. In this chapter we are focused on the power dissipation of the plasma and the influences of impurities on this.

4.1 Basics of electrical power

There are different ways to calculate the power and it is important to know these differences. Most of the time, the power, in watt [W], is calculated by multiplying the current with the voltage.

$$p(t) = i(t) \cdot v(t) \tag{4.1}$$

The formula 4.1 shows how to get the instantaneous power and depends on the time. This is the most general relation and the definition of the electrical power. But we are often more interested in a average power, especially for sinusoidal or periodic signals.

For a periodic signal, it is more common to calculate the power for one period. The equation 4.2 shows how to get this average power. Nonetheless, if we want to use it, we need the analytic equation of the current and the voltage versus time.

$$P_{avg} = \frac{1}{T}\int_0^T p(t)dt = \frac{1}{T}\int_0^T i(t) \cdot v(t)dt \tag{4.2}$$

For a practical case, we use the mathematic equation 4.3 which is fitted for numerical calculations. k is the sample increment and N is the sample numbers for one period. Thus, it is easy to implement this kind of calculation in a numerical calculation software such as Matlab© or Scilab.

$$P_{avg} = \frac{1}{T}\sum_{k=0}^{N} i_k \cdot v_k \tag{4.3}$$

$$P_{avg} = R \cdot I_{RMS}^2 = \frac{V_{RMS}^2}{R} \tag{4.4}$$

$$P_{avg} = V_{RMS}^2 \cdot I_{RMS} \cos(\varphi) \tag{4.5}$$

The equations 4.2 and 4.3 are not the only solution to get the average power and the relation 4.4 shows how to do with the root mean-square current and voltage for a resistive charge. There must be no phase shift. Otherwise you have to use the equation 4.5, with φ the phase shift between the current and the voltage. R is the resistance of the component which we calculate the dissipated power. Equation 4.4 are usually the formulas which are used more often because it is fitted for direct current too. The root mean square current and voltage can be calculated for periodic signals such as sinusoidal signals. The relations 4.6 are the expressions of the root mean square current and voltage respectively. The discrete forms are used for numerical calculations with n being one sample of the whole signal and N being the sample numbers of one period. T is the period time and I_0, V_0 are the current and voltage amplitude respectively.

$$\begin{aligned} I_{RMS} &= \sqrt{\frac{1}{T}\int_t^{t+T} i^2(t)dt} = \sqrt{\frac{1}{T}\sum_{k=n}^{n+N} i_k^2} \\ \text{if i(t) is a sinusoidal signal, } I_{RMS} &= \frac{I_0}{\sqrt{2}} \\ V_{RMS} &= \sqrt{\frac{1}{T}\int_t^{t+T} v^2(t)dt} = \sqrt{\frac{1}{T}\sum_{k=n}^{n+N} v_k^2} \\ \text{if v(t) is a sinusoidal signal, } V_{RMS} &= \frac{V_0}{\sqrt{2}} \end{aligned} \tag{4.6}$$

4.2 Setup and electrical circuit

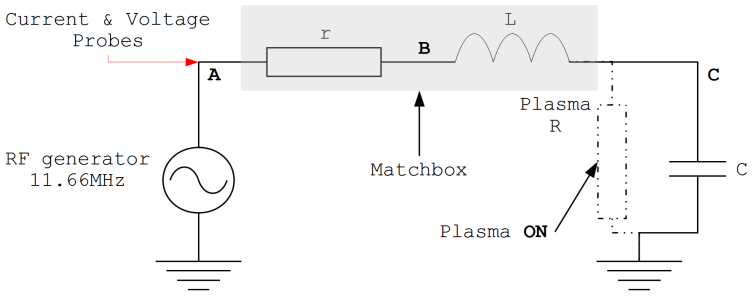

Figure 4.1: Electrical circuit of the RF APPJ from *EPG*.

The plasma jet is connected to a radio frequency amplifier. The RF signal itself is a low voltage high frequency generator and fed to the amplifier. The matchbox is simplified as much as possible in order to reduce the power dissipation in the components that is why there is only a coil inside. The match between the circuit and the plasma is done by adjusting the generator frequency. Instead of using the normed frequency at 13.56 MHz, we use the generator at 11.66 Mhz because at this frequency the least amount of the power is reflected. The current and voltage probes are connected between the generator and the matchbox in order to reduce the capacitive effect and disturbance of the plasma. As the capacity of the plasma is in the same order of magnitude as the plasma source. It changes the plasma characteristics significantly when inserting between the plasma jet and the matchbox.

Figure 4.1 shows the circuit of the setup. We can see the generator, a self-inductance L, a capacitor C where one of its plate is the needle. The resistor r is the sum of all the stray impedance of the matchbox which means the cables and the coil. When the plasma is on, there is a resistor R which is added in parallel with the capacitor. This

deals with the resistive part of the plasma. The probes are connected between the generator and the matchbox in order to minimize the effect on the plasma. The equation 4.7 is a second order differential equation which can be solved in order to know the needle electrode voltage.

$$V_C(t) = LC \cdot \frac{\mathrm{d}^2 V_B(t)}{\mathrm{d}t^2} + \left(\frac{L}{R} - rC\right) \cdot \frac{\mathrm{d}V_B(t)}{\mathrm{d}t} + \frac{r}{R} \cdot V_B(t) + V_A(t) \tag{4.7}$$

The data acquisitions are done with the oscilloscope at the sample frequency of 2 GS/s and we save roughly one hundred periods long. The power is calculated for each period and then it is averaged in order to reduce the error. The error of the I_{RMS} and I_{RMS} is guessed by the statistic calculation of the standard deviation or the variance square root. All those calculations are done with a numerical Scilab[1] program. By this way we can also correct the phase shift induced by the cables. The radio frequencies are sensitive to the capacitive effect in the cables and depends on the length. The current voltage couple is out-of-phase. Normally, the shift between current and voltage is 90° for a capacitive charge. With a vacuum capacitor, we check the phase shift due to the current and the voltage probe and the cables. We get a correction phase shift corresponding to 3.31 ns which means that the voltage is slower than the current. This factor has been taken to account in the numerical calculations.

4.3 Results

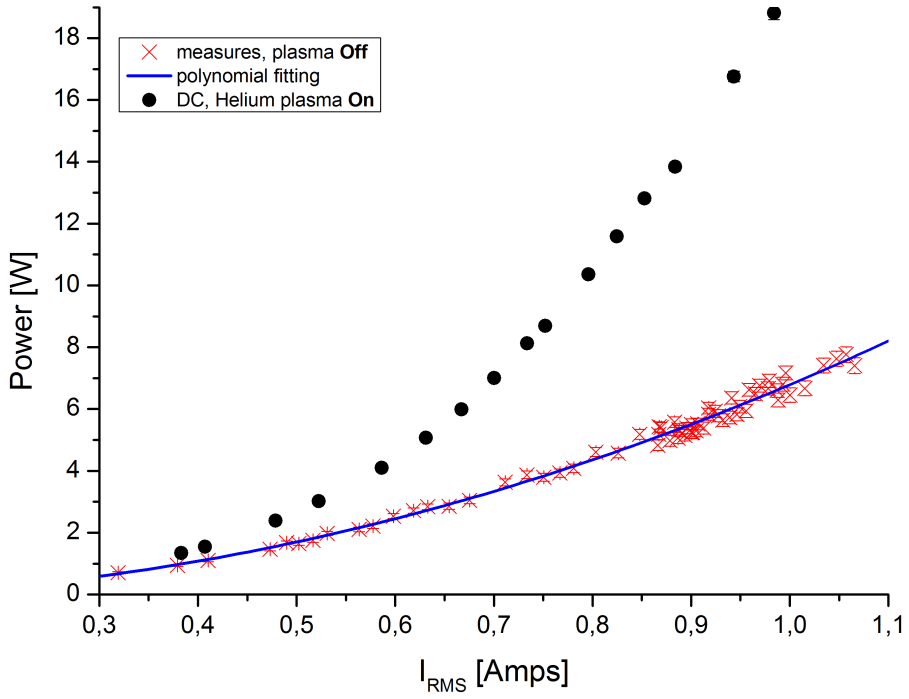

Figure 4.2: Plasma dissipated power calculation method. This example is from a Helium plasma jet without second electrode.

The power that we want to investigate is the power which is dissipated in the plasma. The matchbox consumes a part of the power even when the plasma is shutting down. Figure 4.2 shows the measurements of the power dissipation versus the root mean square current. We can see that these curves seem to follow the quadratic

[1] www.scilab.org/

equation 4.4. The red scatter points show the dissipated power in the matchbox, thus this amount of power is not dissipated by the plasma because these measurements are done with plasma off which means without gas flow. In order to know how big the power dissipated only by the plasma is, we should subtract the plasma off power from the measurements. The black scatter points are the measurements of a Helium plasma. We can see that the total power is higher in this case because of the plasma. Generally, $P_{total}(I_{RMS}) = P_{matchbox}(I_{RMS}) + P_{plasma}(I_{RMS})$. To be more accurate and reduce the errors, we have to subtract $P_{total}(I_{RMS}) - P_{matchbox}(I_{RMS})$ for the same current. One of the solutions is to fit the red scatter points which a second order polynomial model. The blue curve is the plot of the equation 4.8 that we use far power calculations.

$$P_{avg}(I_{RMS}) \approx 6.6239 \cdot I_{RMS}^2 + 0.2427 \cdot I_{RMS} \tag{4.8}$$

4.3.1 Influence of Nitrogen and Oxygen

The figure 4.3 shows the dissipated power in an Argon and Helium plasma. The Helium plasma seems to use more power which goes up faster that Argon.

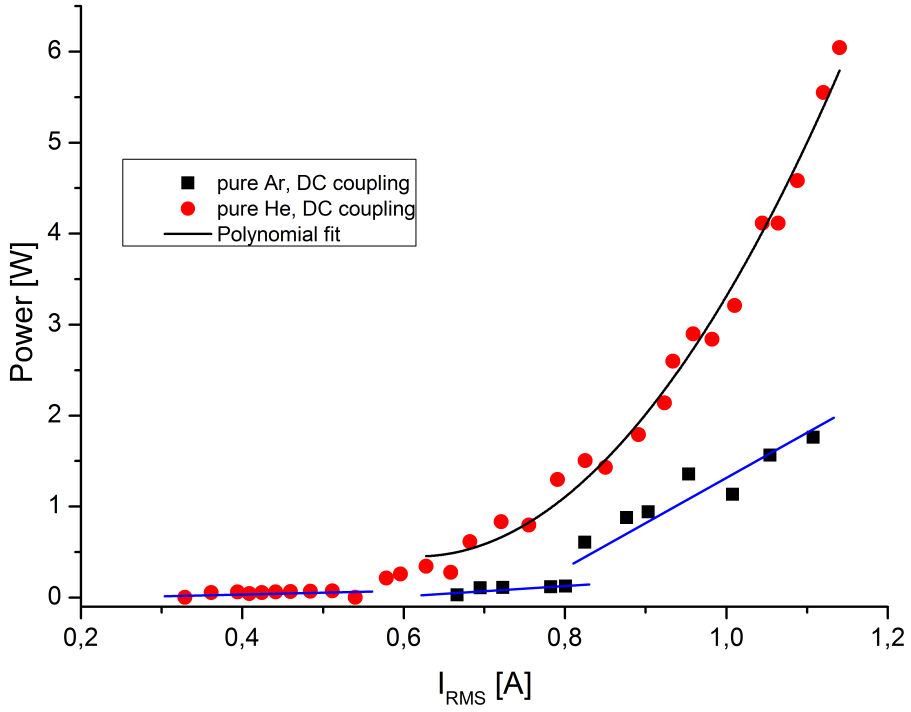

Figure 4.3: Power dissipated by the Argon and Helium plasma jet without second electrode.

The figure 4.4 shows the results of the dissipated power versus concentrations for different gas mixture. These are only the dissipated plasma power. We can see the influence of the Nitrogen and the Oxygen which seem to have not the same behavior in the plasma. The impurity concentrations have also a consequence of the power dissipation. The measurements were done at the same root mean square current, $I_{RMS} = 0.9$ A.

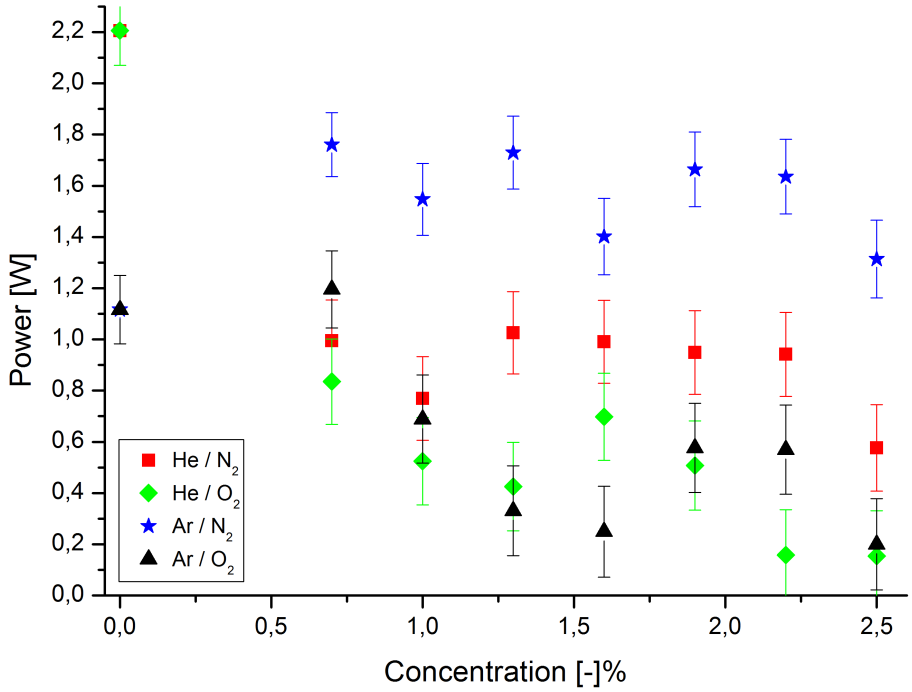

Figure 4.4: Plasma dissipated power for different gas mixtures. For all this measurements I_{RMS}=0.9 A.

4.3.2 Influence of the second electrode

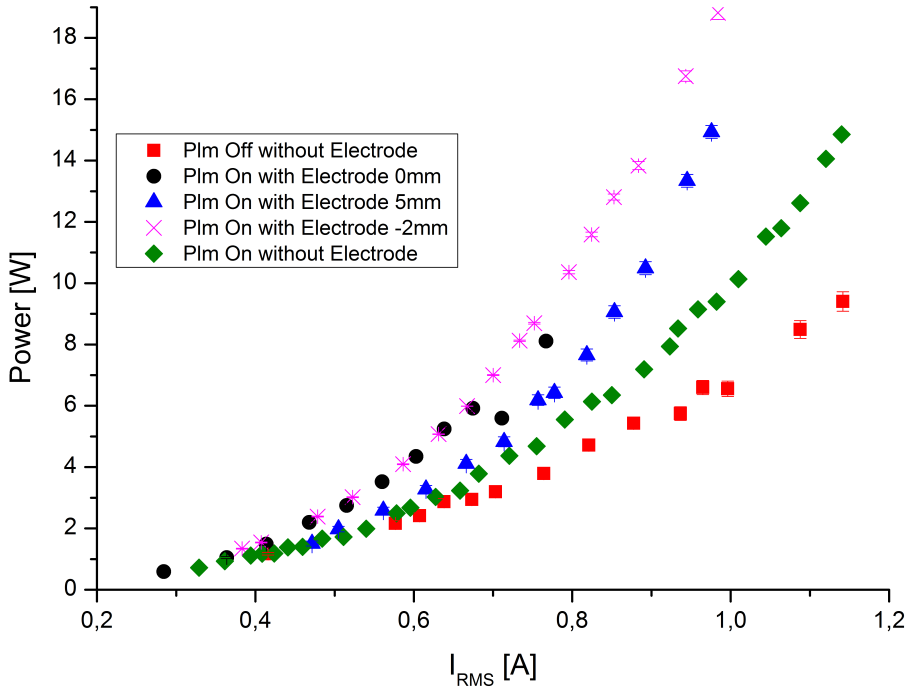

Figure 4.5: Influence of the electrode for the power measurement of a Helium APPJ.

The figure 4.5 shows a graph with five curves which deal with the influence of the second electrode. This one is a grounded copper piece with a 5 mm diameter hole in the middle. The origin for the position is the needle tip. We use a DC-coupling for the oscilloscope because of the offset which can be expected because of the second

electrode.

4.4 Discussion

First of all, the power dissipated in the plasma is different for each gas. From figure 4.3 we learn that Argon and Helium do not need the same power for the same current. From 0.3 to 0.6 A, the power is constant and low for Helium. After 0.6 A the power is going up faster for Helium and it could be because the plasma becomes more resistive. For the second part, the Helium plasma seems to follow the equation 4.4 and is more resistive than capacitive. The phase shift is smaller than 17 degrees. For Argon, the power is quite linear and low if we compare it to the Helium case. The linear fact might be the same state than Helium from 0.3 to 0.6 A. It might be possible to get more resistive Argon plasma but for a higher current and we do not want to go too high otherwise we can destroy the supply and melt the plasma jet. About the power density, we guess that it is roughly the same for both. Looking the figures 2.1 and 2.2 on page 20 and 21 we can see that the Argon plasma is more constrict than Helium. The Helium plasma volume is larger than Argon, but if we calculate the ratio between both, the power density seems to be of the same order of magnitude. Another hypothesis could be that Helium loses more electrons than Argon plasma because of the exchange surface with air. Then, in order to make up for this loss, the power increases. The ionization energy for Helium is also higher than Argon which could explain why the Helium plasma jet needs larger voltage in order to increase the electric field. As a result, the power also increases. The temperature can also play a role but we deal with it in a specific chapter of this report on page 48.

About the impurities and the power change, figure 4.4 shows the power for different gas mixtures and different concentrations. We can see that Nitrogen and Oxygen have not the same influence. Nitrogen seems to make the power constant for Argon and Helium even if at 2.5% the power starts to decrease. For pure Argon, the power seems to be a higher when Nitrogen is added. It is probably because the plasma needs more power to excite and ionize Nitrogen molecules which have roughly the same ionization energy. Thus, a part of energy is lost to dissociate and excite the vobrational and rotational level. The power increases in order to composate all these mechanisms. The jet is more stable and it is similar for the power when we added Nitrogen inside. For Helium, the power is going lower when it is mixed with Nitrogen. One reason could be that Nitrogen and Oxygen help the ionisation process which becomes easier. As a consequence, the voltage drops in order to obtain the same current. The concentration variations do not affect the dissipated power which is around 1 W. We can see a similar behavior between Ar-N_2 and He-N_2 jets. There is a small drop at 1% of N_2 for both cases. Moreover, we can see a similar thing if we look at the mixtures with Oxygen. There is a small increase that we can see for both cases. To add Oxygen induces that the power decreases. We can make a link with the pictures 2.4 and 2.6 on pages 22 and 24 where we see that the plume is going smaller is the Oxygen concentration is increasing. We also notice that even if the Helium power dissipation is higher that Argon, adding Oxygen makes that both have a power dissipation which is roughly the same order of magnitude than the error bar.
About the influence of the electrode, it is expected that there are some changes. The needle electrode is playing one plate of the capacitor and the second electrode is playing the other plate. The capacity is sensitive to the distance between the plates. Figure 4.5 shows how big the influence of the second electrode on the plasma jet is. This second electrode is a plane copper piece of 2 mm thick and with a 5 mm diameter whole in the middle. It is grounded. We can see that when the electrode is around the needle, the power is going up faster than without. Nevertheless there is no big change if the electrode is around the needle or just at its tip. We just get a spark if the voltage is too high when the electrode is at the tip while it is impossible when the electrode is around the electrode because of the glass tube between both. For the next measurements we have to take care of the position of the

electrode and to use it for the same conditions in order to get the same results and do not change the plasma.

Chapter 5

Investigation of the temperature

In plasma physics and especially for Atmospheric Pressure Plasma Jets, the temperature is one of the most important factors. An application of this kind of plasma is to treat wounds thus the plasma jet must be compatible with tissues which means that the gas temperature has not to be too high. The accurate diagnostic of this parameter is not easy to do. The plasma can react by different ways such as the electric field, the charges, the chemical process,... A non-invasive method to investigate is the radiative emission of the glow. By this way, it will be possible to have a good idea of the gas temperature.

5.1 Boltzmann plot Theory

In most cases, APPJs are not at the thermodynamical equilibrium. Nonetheless the energies of the different degrees of freedom (rotational, translational, ...) of different species are normally close to the equilibrium and follow a Boltzmann low. The equation 5.1 is the general form of the Boltzmann law with N_i and N_j the particule density in the quantum state i and j respectively for the up and low energy, g_i and g_j are the statistic weights of each energy level and k_B is the Boltzmann constant. T_{rot} is the rotational temperature of the molecules. Because of the relatively high pressure which means that there are lots of collisions and a fast thermalization of the rotational energy levels. It should be close to the gas temperature that is why this technique is used.

$$\frac{N_j}{N_i} = \frac{g_j}{g_i} \cdot e^{-\frac{E_j - E_i}{k \cdot T_{rot}}} \tag{5.1}$$

From this property it is possible to make a link between the emission intensity ε_{ij} of the line at the wavelength λ. The equation 5.2 shows how the emission intensity is proportional to the rotational temperature.

$$\begin{gathered} \varepsilon_{ij} = \frac{hc}{4\pi\lambda} \cdot \frac{N(T_{rot})}{Q(T_{rot})} \cdot A_{ij} \cdot e^{-\frac{E_j - E_i}{k_B \cdot T_{rot}}} \\ \text{with} \\ Q(T_{rot}) = \sum_i g_i \cdot e^{-\frac{E_i}{k_B \cdot T_{rot}}} \end{gathered} \tag{5.2}$$

The $N(T_{rot})$ and $Q(T_{rot})$ are the total number of particles or the particle density and the partition function respectively. A_{ij} is the first Einstein coefficient, h is the Planck constant. It is possible to write this one to another form in order to have an easier way to calculate T_{rot}. The equation 5.3 can be used to find the rotational tempera-

ture because it is a linear equation.

$$\ln\left(\frac{\varepsilon_{ij}\cdot\lambda}{g_i\cdot A_{ij}}\right)=\frac{-E_i}{k_B\cdot T_{rot}}+\ln\left(\frac{hc\cdot N\left(T_{rot}\right)}{4\pi\cdot Q\left(T_{rot}\right)}\right) \tag{5.3}$$

The first term is inversely proportional to T_{rot} and also the coefficient of the slope. The second does not depends on the energy, thus we do not have to know the expression of $N\left(T_{rot}\right)$ and $Q\left(T_{rot}\right)$. Figure 5.1 shows the appearance of a Boltzmann plot.

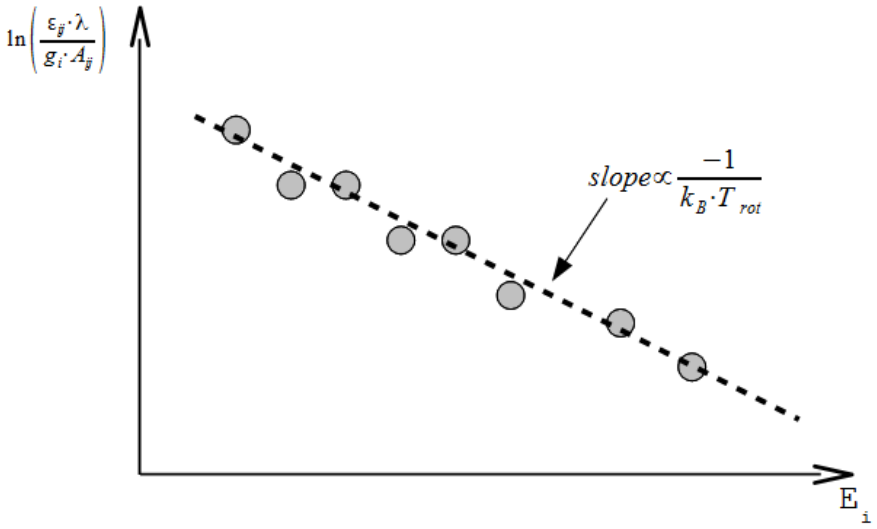

Figure 5.1: Schematic Boltzmann plot for different rotational energy level.

In order to get a accurate value of the temperature and to minimize the error size, there are three conditions which have to be respected for the measurements.

- The peak should be isolate and easily detectable,
- The auto-absorption has to be weak for the peak,
- To know with a good accuracy the emission probability coefficient A_{ij} of the peak.

For this investigation we choose to use the OH(A-X) rotational lines for many reasons. The physical mechanism is well known for this transition and the intensity of this peak is quite high relatively which reduces the errors. This element has also a good sensibility of the temperature changes and is detectable with a common monochromator.

5.2 Setup and measurements

The experimental part is reduced to a spectrometry measurement. The conditions are similar to the previous one and described in the chapter 3, section 3.2 on page 28. The main difference is the spectrometer which has a smaller range but a higher resolution. This spectrometer is a Jobin Yvon monochromator with 22 pm of resolution. The image of the spectrum is taken with a Santa Barbara Instrument Group CCD camera. As we said before, the element transition which is used for the Boltzmann plot is OH(A-X) at 309 nm. In order to calibrate the wavelength scale, we use a Hg lamp and the peaks at 312.5674, 313.1555 and 313.1844 nm because they are the closest peaks to the OH(A-X) one. The amplitude sensibility is also calibrated for the range around 310 nm with a deuterium

lamp. It enable us to for the wavelength sensitivity of the spectrometer.

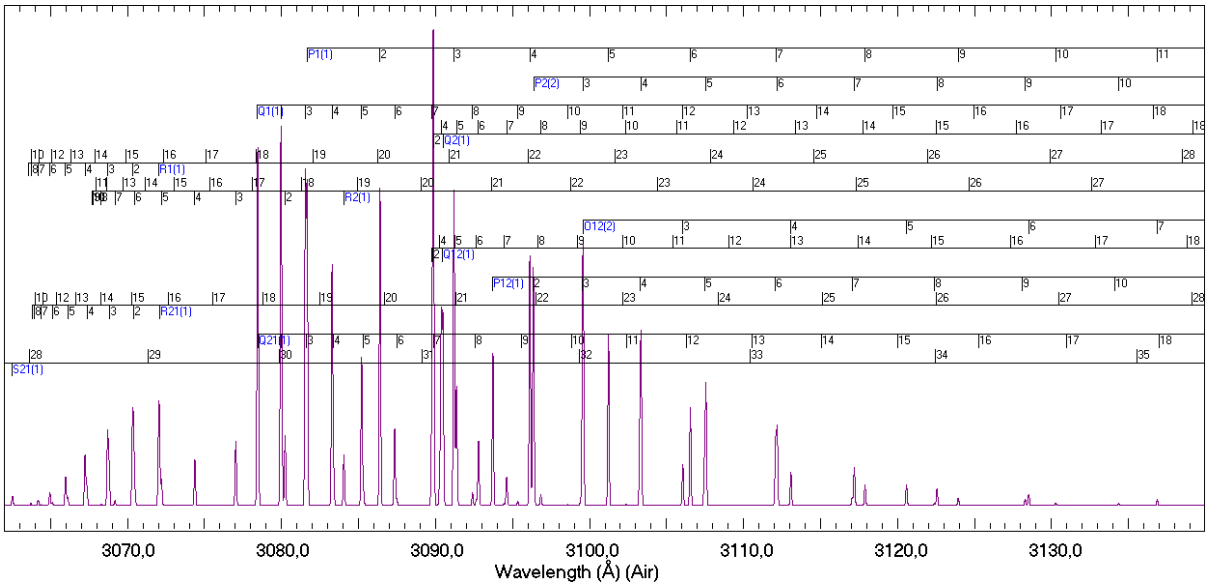

Figure 5.2: Lifbase simulation of the OH(A-X) spectrum from 306 to 314 nm at 400 K.

Figure 5.2 is the spectrum of OH(A-X) with the rotational branches. We can see that the spectrum is centered on the vibrational energy level at 309.0575 nm. This peak has the highest intensity and is called band head. Because of the temperature and the electron energies which are shared by the Boltzmann distribution, all the peak intensities change. As a result, the energy of each of them is also changed when the temperature changed.
About the experimental procedure, we want to know how the temperature evolves along the plasma jet for pure Argon and Pure Helium plasma. We probe the jet each 2 mm from the needle tip to the end of the plume. For the different mixture such as Ar-N_2, Ar-O_2, and He-N_2, He-O_2, we probe the temperature at the needle tip only but for different concentration in order to know how big the influence of the impurities are.

5.3 Post processing, options and constructing the Boltzmann plot

The Boltzmann plot is a good method to set an idea of the gas temperature but it has to be used with care in order to restrict the error. According to [20] the equation 5.3 on page 49 can be written with some other parameters such as B_ν as the rotational constant or J and J' as two different rotational energy levels. Thus equation 5.3 became:

$$\varepsilon_{JJ'} \propto h\nu_{JJ'}\,(2J+1)\,A_{JJ'}\,e^{-\frac{B_\nu hcJ(J+1)}{k_B T_{rot}}} \tag{5.4}$$

It is also important to make sure of the intensity of each peak. They have to be isolated. Otherwise, we do not know how big the peak intensity is due from one rotational energy transition. According to the Lifebase simulation on figure 5.2, all the rotational energy emission lines have been checked and we keep only the ones that we are sure of their contribution for the emission peak intensity. The table 5.1 holds the information about all the peaks which are used for the Boltzmann plot.

Branch	J	Wavelength cm^{-1}	Wavelength nm	$A_{JJ'}$ [21]	2J+1 [22]	E_i [22] cm^{-1}
P1	2	32390,92	308,72	671	3	32474,62
	5	32235,96	310,21	501	9	32779,49
	6	32180,83	310,74	481	11	32948,31
	8	32063,72	311,87	449	15	33384,97
	9	32001,56	312,48	435	17	33652,29
	10	31936,84	313,11	421	19	33951,8
P2	6	32122,56	311,3	440	11	32947,05
	9	31957,2	312,91	420	17	33650,38
	10	31895,41	313,52	410	19	33949,67
	11	31830,53	314,16	401	21	34280,64
Q1	5	32403,47	308,6	724	11	32948,31
	8	32328,06	309,32	739	17	33652,29
	9	32297,38	309,62	734	19	33951,8
	10	32263,45	309,94	726	21	34282,99
	13	32142,7	311,11	686	27	35462,01
Q2	7	32304,79	309,55	735	15	33383,26
	11	32189,94	310,65	722	23	34642,92
	12	32151,9	311,02	711	25	35035,86
R2	1	32415,51	308,49	140	5	32541,98
	3	32489,49	307,79	239	9	32778,49
	4	32517,58	307,52	269	11	32947,05
	7	32572,59	307	316	17	33650,38
	8	32582,11	306,91	322	19	33949,67

Table 5.1: Wavelength of the rotational energy emissions used for the Boltzmann plot and the constants needed.

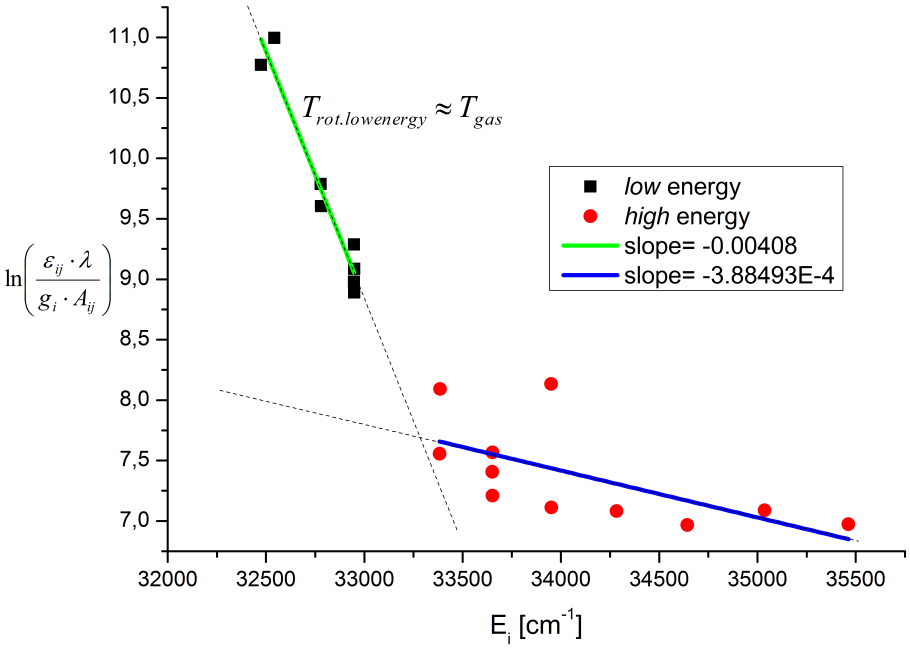

Figure 5.3: Experimental Boltzmann plot from OH(A-X) rotational energy for Helium Nitrogen APPJ at 400 K.

Figure 5.3 is a Boltzmann plot of a Helium plasma with 2.5% of Nitrogen plasma jet. We can see that the curve is not linear as expected for a rotational population distribution in equilibrium. It is clear that if we calculate a linear regression with all the data points the result will be an overestimation of the gas temperature. We should split the scatter of points in two parts in order to reveal two segments. The green one has the steepest slope and corresponds to the lower rotational energy levels which should correspond to the gas temperature. The other part of the graph refers to another temperature which depends strongly on the plasma conditions and the production process of OH(A), especially for the atmospheric pressure. This is the consequence of the deviation from the Boltzmann distribution and the non-thermodynamical equilibrium. A thorough analysis of the second temperature is outside the scope of this work.
The following temperatures that we will assume for the next part of this report are calculated with only the first 5 rotational levels of each branch in order to avoid influence of the high rotational excitation in the temperature determination. But this temperature might be not the real gas temperature because of the over estimation of the Boltzmann plot and we have to keep it in mind for the rest of the diagnostic. With this technique, it is difficult to have an error smaller than ± 50 K.

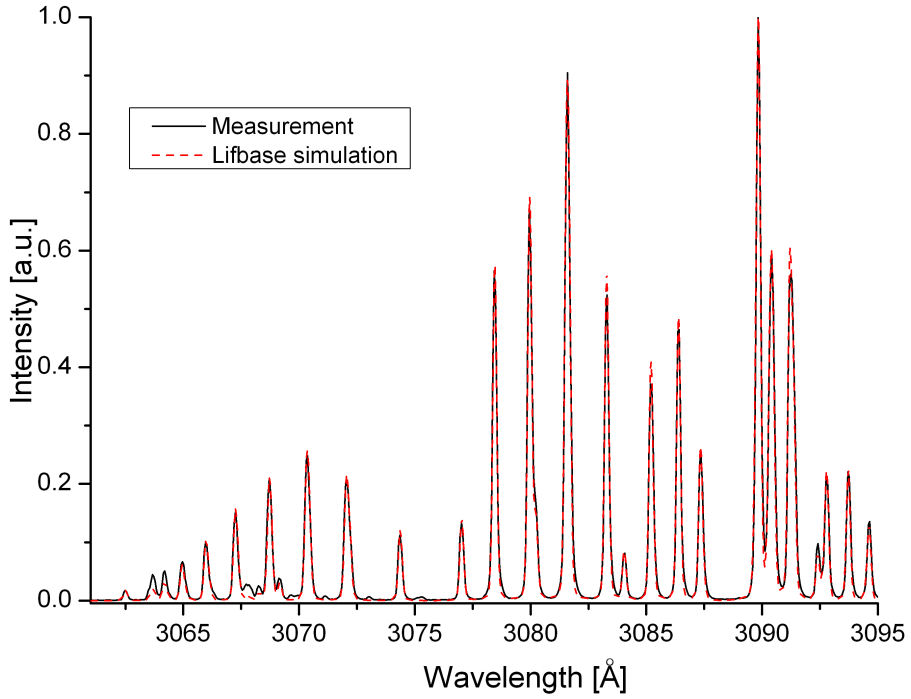

Figure 5.4: OH(A-X)(0-0) (309 nm) measured for a pure Helium plasma jet and Lifbase simulation spectrum at 400 K.

Another solution to know the rotational temperature is to use a spectrum simulation software such as Lifbase. This method is to find the best fit between experimental spectrum and simulated spectrum. Figure 5.4 is an example of fitting. We can see that the fit is quite good which means that the rotational temperature should be similar too. In getting the best fit, we refer to two statistical parameters which are the correlation factor and the root mean square error. Note that it is clear that the high rotational excitation (contribution for the second temperature) does not affect a lot the fitting of OH(A-X) spectrum. For all the spectra that we fit with the simulations we can assume that the correlation factor is over 0.99. Then, to get a better result, we optimise the fit in order to minimize the root mean square error. The tables 5.2 and 5.3 contain the root mean square error for all the spectra. By this value we

can have a idea of the temperature error.
Finally, we will use the rotational energy lines of N_2 at 309 nm and N_2^+ at 391 nm to get another estimate of the gas temperature and to check if it is the same order of magnitude of the Boltzmann plot temperature. We compare the experimantal spectra to the simulation from Specair.

5.4 Results

5.4.1 Rotationnal temperature of OH(A-X): Botltzmann plot and spectrum simulations

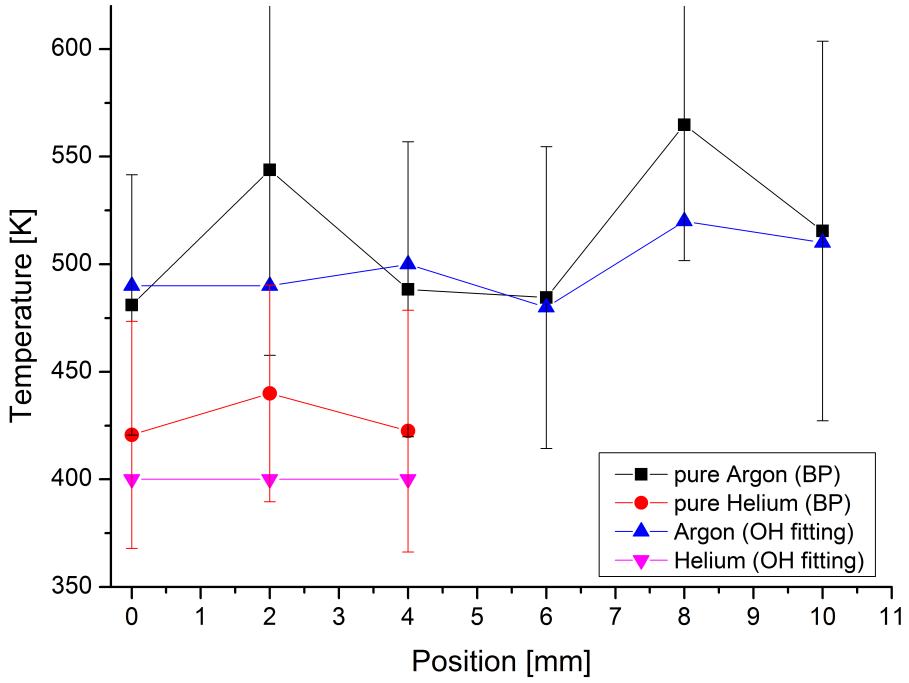

Figure 5.5: Pure Argon and Helium plasma jet OH rotational temperature for different position from the needle electrode. *BP* and *OH* fitting mean that the temperature is estimate by the Boltzmann plot and the fitting respectively.

The first experiments about the temperature estimation are focused on the temperature distribution along the jet. Figure 5.5 is a graph which represents the rotational temperatures of OH(A-X). It deals with pure Argon and pure Helium plasma jets and shows the results of two different techniques. For both gases, the temperature is quite stable. Argon temperature is also a bit higher of 80 K than Helium. The black scatter points are the temperature estimation from the Boltzmann plot. The average error is around 70 K but you can see all the details in the table 5.2. We can assume that the Argon temperature is constant along the jet and is around 500 K. The OH(A-X) fitting spectra gives the same trend and the temperatures which are measured by this technique is close to the ones that are calculated by the Boltzmann plot.
About the Helium, the results are similar which means that the temperature is constant along the jet. The Boltzmann plot and the simulation are consistent. The temperature of the Helium jet is around 410 K. The table 5.2 indicates all the temperatures, the errors and the parameters for both techniques.
We investigate the influence of Nitrogen and Oxygen mixtures on the temperature.

Figure 5.6 and table 5.3 give many results from the measurements. From the graph we can see that the Helium temperature does not change too much and the average is around 360 K. Nitrogen is just dropping the

Position mm	Slope $m^{-2}.kg.s^{-2}$	Slope Error $m^{-2}.kg.s^{-2}$	Error %	T. Boltz.plot K	Error ΔK	T. Fit Lifbase K	χ^2 .
Pure He							
0	-0.00342	0.000429	13	420	50	400	7
2	-0.00327	0.000375	11	440	50	400	7
4	-0.00341	0.000453	13	420	60	400	8
Pure Ar							
0	-0.00299	0.000376	13	480	60	490	7
2	-0.00265	0.000419	16	540	90	490	8
4	-0.00295	0.000414	14	490	70	500	8
6	-0.00297	0.00043	14	480	70	480	7
8	-0.00255	0.000285	11	560	60	520	8
10	-0.00279	0.000478	17	520	90	510	13

Table 5.2: Temperatures for different positions of an Argon and Helium plasma jet.

temperatures but they are still constant. As before, the Boltzmann plot and the simulation seem to give quite similar temperatures even if the Boltzmann plot temperature is higher than the simulation. About the Nitrogen influence with Argon mixture, it is difficult to have a clear idea of the temperature. The Boltzmann plot is not able to give us accurate temperatures. If we look at the table 5.3, we can see that the errors are bigger than previously but the temperature that we find could be realistic. It is even difficult to have an idea of the temperature stability along the jet because of the simulation fitting results. It seems that it is the opposite, and the simulation gives a higher gas temperature. But it is constant around 500 K which is quite similar than pure Argon plasma jet. The only thing which is coherent between the two methods for the Argon Nitrogen mixture is the errors. The slope errors are bigger than the previous cases and the χ^2 is bigger too.

About the Oxygen influence, it is also difficult to have a clear idea for many reasons. As we said before, increase of the Oxygen concentration reduces the jet length, so it is more difficult to have a good spectrum and the OH emission is also going smaller. From the table 5.3 we can assume that the Oxygen reduce the temperature of the jet. The errors are also quite high and it is difficult to have a good estimation of the temperatures. We just can assume that for the Helium-Oxygen mixture, the temperature from the Boltzmann plot and the simulation match well. Thus the Helium Oxygen plasma jet is around 390 K and the Oxygen concentration seems to play a minor role to change the gas temperature.

5.4.2 Rotational temperature of N_2 (337) and N_2^+: spectrum simulations

We also look at the rotational temperature of N_2^+ (391 nm) and N_2 (337 nm). The peak intensities are quite low, thus the noise is more present in the spectra. The table 5.4 shows the results of the spectrum simulations with the Specair software. First, the fitting is more difficult to do than with OH(A-X) because of the noise and the small wavelength shift of the experimental spectra. We try to use these elements to have an idea of the gas temperature and we can see that the order of magnitude for the He-N_2 mixture is roughly similar if we consider the error which is larger. The fitting with the simulations was done for the possible cases, thus it is impossible for us to use the Argon spectra because they do not match with the simulations. The main reason is that there are some other peaks which disturb the reading of the rotational band of N_2. N_2^+ peak is too small to get a good signal even with 300 s of exposure time.

Position %	Slope $m^{-2}.kg.s^{-2}$	Slope Error $m^{-2}.kg.s^{-2}$	Error %	T. Boltz.plot K	Error ΔK	T. Fit Lifbase K	χ^2 .
He-N_2							
0.7	-0,00380	0,00041	11	380	40	380	19
1.3	-0,00370	0,000471	13	390	50	350	21
1.9	-0,00370	0,000731	20	390	80	350	22
2.5	-0,00410	0,000387	9	350	30	350	23
He-O_2							
0.7	-0,00380	0,000434	12	380	40	350	15
1.3	-0,00260	0,00228	86	540	470	350	49
Ar-N_2							
0.7	-0,00320	0,0039	123	450	560	470	19
1.3	-0,00390	0,00357	92	370	300	520	21
1.9	-0,00360	0,0034	95	401	381	520	21
2.5	-0,00530	0,00342	64	270	170	500	20
He-O_2							
0.7	-0,00350	0,003813	108	410	440	380	13
1.3	-0,00370	0,000444	12	390	50	400	19
1.9	-	-	-	-	-	400	23

Table 5.3: Temperatures for different Nitrogen and Oxygen concentrations mixed with Argon or Helium plasma jet. The measurements are done just at the needle tip.

concentration %	N_2^+ (391 nm) K	error ± K	N_2 (337 nm) K	error ± K
He-N_2				
0	420	30	330	60
0.7	360	30	300	60
1.3	380	30	290	60
2.5	415	30	250	60
He-O_2				
0.7	340	30	280	60

Table 5.4: N_2^+ and N_2 rotational temperatures for different Nitrogen and Oxygen concentration mixed with Helium plasma jet. The measurements are done just at the needle tip.

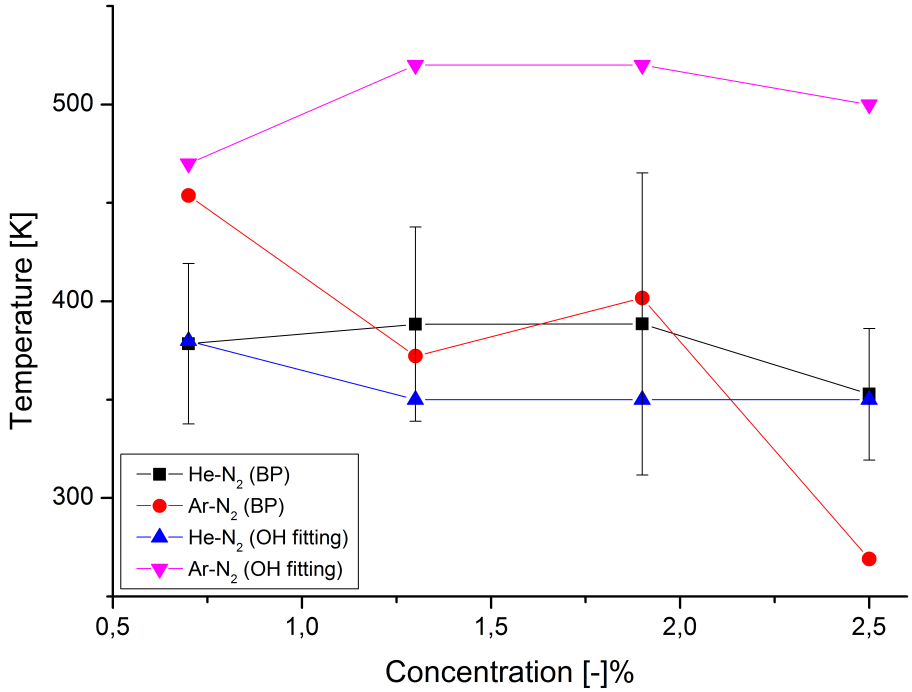

Figure 5.6: OH rotational temperature for different gas mixture concentrations with Argon and Helium. The errors for the Ar-N_2 gas temperature from the Boltzmann plot is not drawn because the values are to big to be realistic.

5.5 Discussion

The temperature and the power are good parameters to investigate the plasma and to get information about the plasma behavior. As we can expect from the Nitrogen influence on the dissipated power in the plasma jet, Nitrogen is not influencing the Helium plasma when it is mixed with it. Figure 4.4 on page 45 evince that the power is constant in the range of 0 to 2.5% of N_2. This behavior is similar for the temperature because it is also constant which means that Nitrogen does not change the energy balance. On the other hand Helium plasma jet dissipates more power and we could expect that it produces more heat. We cannot assume this, but we already know that pure Argon plasma jet is hotter than Helium. Argon plasma dissipates also less power. This contrast could be explained by the higher thermal conductivity factor of Helium which can lose more heat with surround air. According to the chapter 2, section 2.3.1 on page 20, Argon plasma is more constricted and looks like a filament which can concentrate the heat flux in this area. For Helium the heat flux might be similar but as the jet is more diffuse, the heat density is lower. This has to be checked by investigated further.

About the Oxygen influence, it is more difficult to have an idea because of the contrast between the power dissipation in the plasma and the temperature. Looking at the figure 4.4 on page 45, as the power is decreasing with increasing Oxygen concentration, we could expect the same behavior for the temperature. From the measurements and the simulations that we have done, the temperature seems to be constant, at least the decay is more dominant for the power than for the temperature even if we take into account the errors. This means that the energy seems to be lost by another mechanism as the thermal transfer.

Chapter 6

Plasma jet in contact with distilled water and saline solutions: first investigations

Through the previous chapters, we have investigated some characteristics of the Helium and Argon APPJ. In these experiments, the plasma jet has only interaction with air. In order to go further and look at the plasma jet behavior we decide to do some experiments with liquid solutions. The future applications of this kind of plasma jet may be the biological interaction and medicine treatments. In these conditions, liquid and salts are unavoidable that is why we look into the plasma jet in specific simple cases such as distilled water and saline solutions.

6.1 Setup and experimental procedure

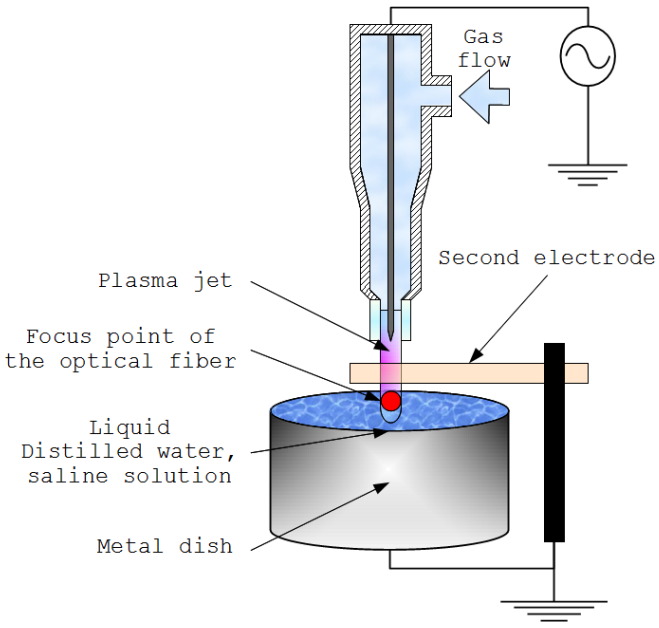

Figure 6.1: Experimental setup of the liquid plasma jet contact experiments.

The plasma jet setup is roughly the same that we describe figure 1.7 on page 17. For the following experiment we just consider the Argon and Helium gases because to introduce Nitrogen and Oxygen effects must be too much experiments and we have not enough time for this. Figure 6.1 shows the complementary components for the tests

with liquids. We can see that the liquid is contained in a metal dish in order to reduce the charge effect. The gas flow is still 1 slpm. One parameter which is extremely important is the distance between the needle and the liquid surface. For the same reason as the second electrode, here the liquid plays a second electrode role. It means that the one behavior part of the plasma seems to be capacitive. If the distance between the needle and the water surface changes we cannot compare the experiment that is why we decided to fix the distance at 5.0 mm. This distance is a good balance because we can access the no-contact and the contact state. The gap is checked before to start each measurement.
During these experiments we also are looking at the influence of the second grounded electrode as discussed in chapter 4, section 4.3.2 on page 45. The second electrode is situated 2 mm from the needle and 1 mm from the liquid surface. Half of the experiments are done with second electrode but the other half is without in order to compare to the previous results such as the power and the temperature. But for the future applications it will be necessary to use a second electrode to be safe.
The nature of the solution is also investigated and we use distilled water and different concentration of KCL solutions. The aim is to change the solution conductivity and to observe if there is some changes in the plasma. The conductivity range is chosen close to the skin conductivity according to [23, 24, 25, 26] from 0.1 to 10 mS and measured with a conductivity meter. The solution could influence the plasma and the chemical reactions that is why we looked into this.

6.2 Macroscopic observations of the plasma jet

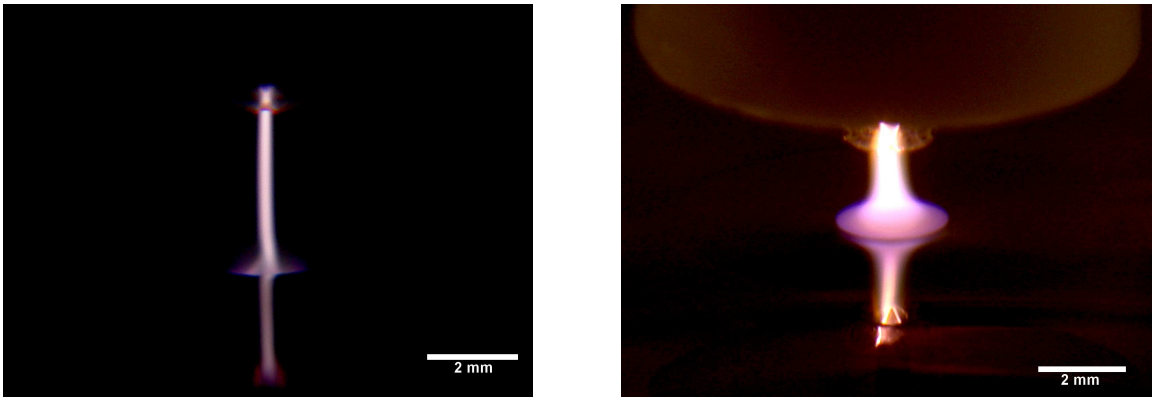

(a) Argon plasma jet connected to the distilled water surface. 1/125 s exposure time.

(b) Helium plasma jet connected to the distilled water surface.1/30 s exposure time.

Figure 6.2: Pictures of an Argon and Helium APPJ connected to a liquid surface.

Before to start the measurement, we look at the macroscopic plasma behavior. It is essential to do if we want to investigate more and know if some diagnostics could be possible. We take this opportunity to take some pictures such as the two which are presented on figure 6.2. We can see two different plasma jets connected to the distilled water surface. The pictures are taken with a 45° angle in order to see the plume but also the contact area shape between the plasma and the liquid. We can notice clearly that Argon, figure 6.2a, and Helium, figure 6.2b plasma jet have not the same behavior: Argon is really filamentary and Helium is more diffuse and the edges of the plasma part which is in contact are smooth. Argon is connected to the liquid by only one thin filament whereas the Helium plasma jet seems to be homogeneous and spreads on the liquid surface. Due to the filamentary jet, the Argon plasma is much brighter than Helium. In the case where the Helium plasma is close to the surface but not

connecting, we can see a sheath less than 0.5 mm thick. Due to the sheath definition, there is no emitting light from this area and the high contrast with the plume are not able us to take a picture of it.

6.3 Influence of the solution conductivity and the second electrode on the power

For the power measurement, it is important to ground everything which is not linked to the generator. The metal dish is grounded in order to let it discharge. We also use a second electrode which is grounded too. Figure 6.3 shows some curves which refer to different configuration. We can see clearly that there is no influence of the conductivity of the solution between the powers. The distilled water has a electrical conductivity below 0.01 mS, which is the minimum conductivity that we can measure with our conductivity-meter. Even for the highest solution conductivity, the power is similar. Thus we can assume that for Helium plasma jet, the solution conductivity does not play a big role on the dissipated power in the plasma. From our diagnostics, it should be the same for Argon. Actually, there is a charge effect when we are measuring the voltage of the Argon plasma jet. It means that some charges stay somewhere in the circuit which increases the needle potential. We notice that there is no problem when the plasma is not connected with the liquid but when it is, the voltage is going up and we can not be sure of the power. It is for this reason that all the measurement series have not the same sample number. We stop to measure when the charge effect is happening. To calculate the power we need good measurements of the voltage and current. But the measured voltage is influenced by some charges which have some difficulty to circulate. As a consequence, the voltage measurements have an off-set which distort the measurements with the oscilloscope. For this reason, it is impossible for our setup to assume a Argon plasma jet dissipated power as accurate as the Helium plasma jet.

Figure 6.4 shows some curves which deal with the second electrode influence on the power. We can see a slight difference between the power curves without using electrode and with electrode. The electrode seems to play a role and the plasma dissipates more power. Nonetheless, it is difficult to give an accurate value but the difference is noticed and higher than the error bars. The solution plays also a role and we can see that the power is increasing faster when we use the second electrode and the solution. Again, the charge effect is happening that is why the blue curve has less samples than the other cases. All these curves look quite linear which means that the plasma is not completely resistive. But during the measurements, we can see with the oscilloscope that the plasma is being more resistive and it is shown by the phase shift which is close to zero between the current and the voltage.On figure 6.5 we can see this phenomenon for the Helium plasma jet. When the plasma is not connected to the liquid, it is more capacitive but when it is connected, we can see that it is only resistive. It is also possible to see the same behavior with the Argon plasma but it is instable due to the filament which changes the contact point every time. This full resistive mode means that the reflected power is lower and also the power is being really high because it is proportional to the square current[1]

6.4 Emission spectroscopy investigation

We use a spectrometer Ocean Optics© HR 2000[2] in order to look into the UV spectrum. The optical fiber is focused on two different positions: at 2 mm and at 5 mm from the needle in order to have an idea of the plasma itself and the intersection with the liquid. We decided to use distilled water in order to avoid the reaction with K, Cl and Na which could add some noise. But it will be necessary to do this kind of test later.
The figure 6.6 shows four normalized spectra for pure Argon APPJ. Each spectrum is corrected for the wavelength

[1] see relation (4.4) on page 41.

[2] The main characteristics are sum up in the table 3.1 on page 28.

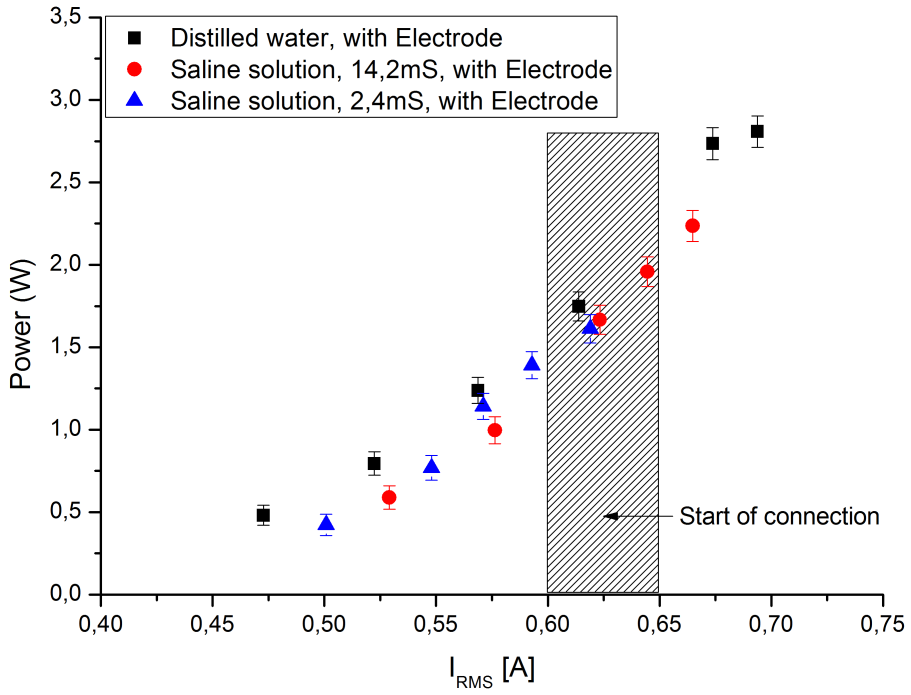

Figure 6.3: Dissipated power Helium plasma jet for different solution conductivities.

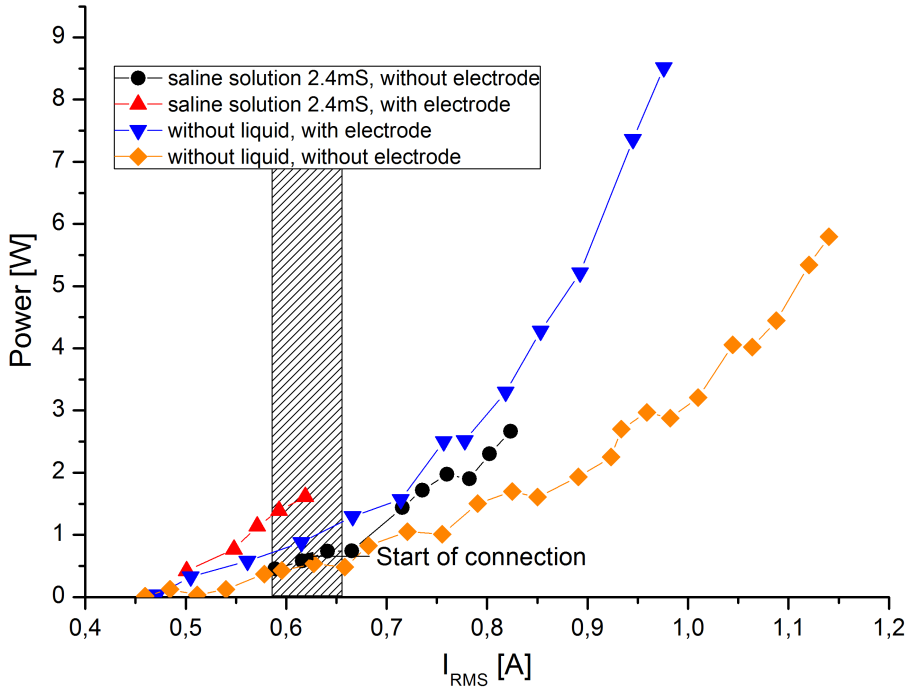

Figure 6.4: Influence of the second electrode on the power for a Helium plasma jet in conatct with saline solutions.

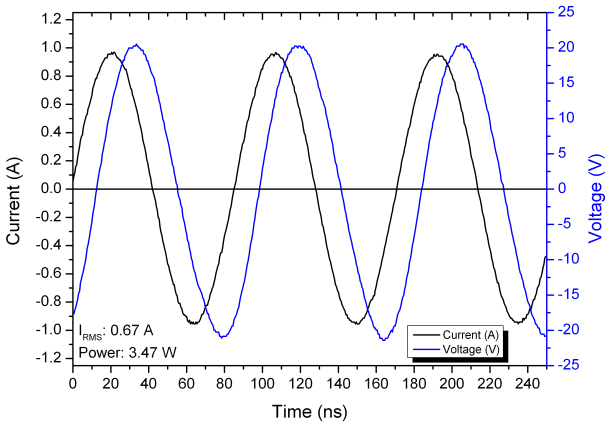

(a) Capacitive mode of the Helium plasma when it is not connected to the liquid.

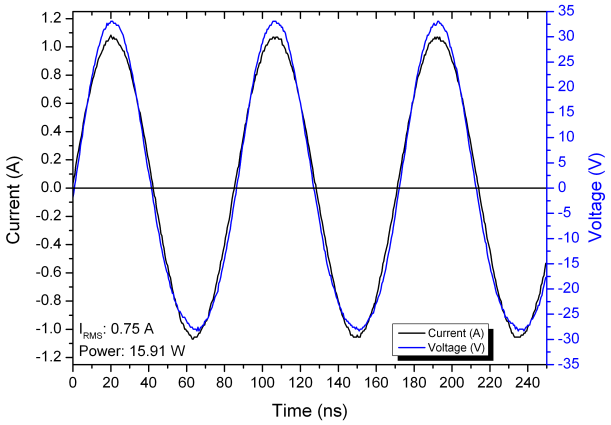

(b) Resistive mode of the Helium plasma when it is connected to the liquid.

Figure 6.5: Helium plasma jet oscillograms for the capacitive and resistive modes.

sensitivity of the spectrometer. We notice that when the plasma is connected, the OH peak at 309 nm is the highest at 2 mm from the needle. But at the surface (5 mm), this peak almost disappears. The Nitrogen molecules are more excited because their emissions at 337 nm are higher. We can assume that because of the exposure time of both are roughly similar and around 28 ms. For the cases where the plasma is not connected to the liquid, the Nitrogen excitation seems to be higher too. In this case, the exposure times are different and the intensity from the liquid surface is four times higher than in the middle of the plume. It means that the N_2 excitation is more important in the area close to the liquid. We could expect the other way round because water is made of Oxygen and Hydrogen thus OH could be more present close to the surface instead of inside the jet a few millimeters higher.

The figure 6.7 shows four normalized spectra of pure Helium APPJ. The experimental procedure are similar to the previous one. For the two cases where the plasma is connected, we can see that the highest peak is OH for the spectrum from 2 mm. But close to the liquid, the OH emission almost disappears and Nitrogen is more excited as the Argon case. For the disconnected cases, we can see that close to the liquid surface the Nitrogen is also highly excited and OH emission is very low. The big change between Argon case and Helium is that at 2 mm when the plasma is connected, the OH emission is quite high. It means that OH emission disappear from 3 mm to 5 mm. The OH emission might be auto-absorbed by the plasma itself in this area.

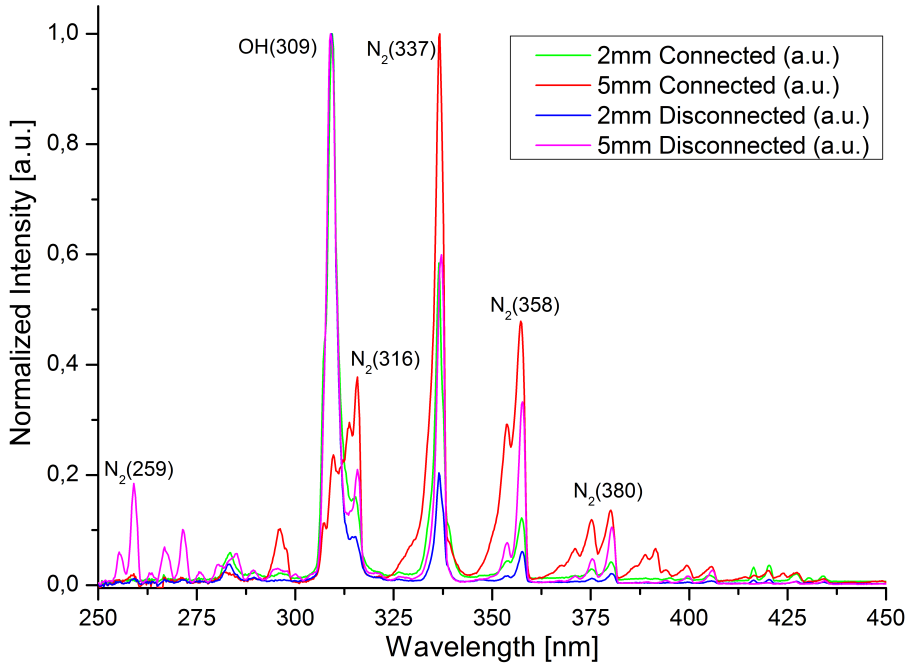

Figure 6.6: Liquid plasma interaction. Argon plasma jet spectra for two different positions from 250 to 450 nm.

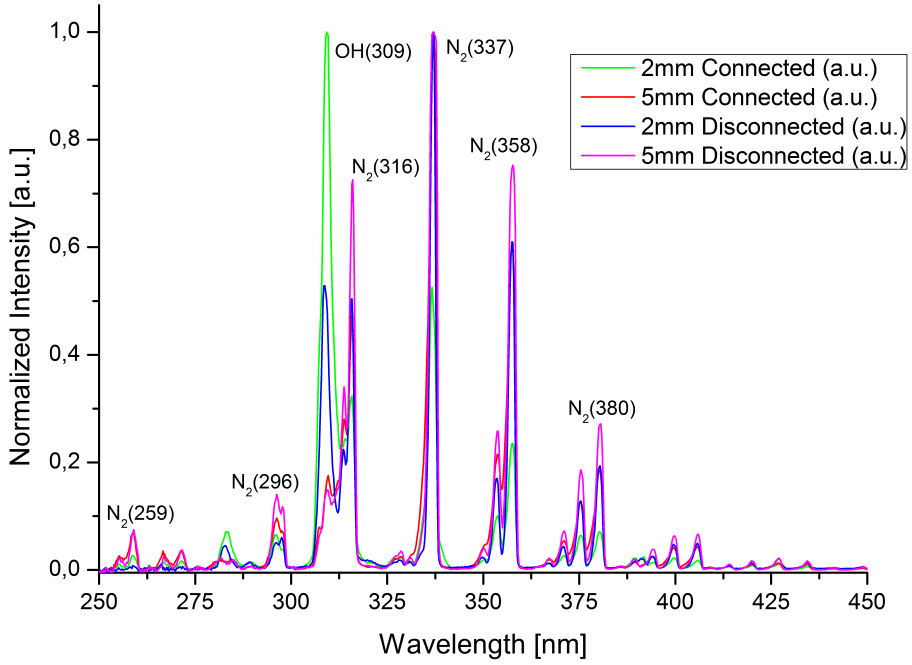

Figure 6.7: Liquid plasma interaction. Helium plasma jet spectra for two different positions from 250 to 450 nm.

It can be useful to continue this diagnostic with looking into the range from 600 nm to 900 nm. We can assume that for the range 450 nm to 600 nm there is no transition line that is why the graphs are reduce to 450 nm.

6.5 Temperature estimation with OH(A-X) fitting with simulation

The temperature of the jet is important, especially when the plasma is connected to the liquid surface. As the good result from the investigation of the plasma jet itself, we decide to use the OH(A-X) rotational energy spectrum to have an idea of the gas temperature.We use the simulation and try to find the best fit of the experimental spectra with the simulation spectra in Lifbase. This method is quicker and the errors are close to the Boltzmann plot in our case. As before, we use the same criteria to estimate the error and the correlation factor is always close to 0.99. The most important part is to minimize the χ^2 and that is what we do here. The optical fiber with a lens is focused on the plasma 2 mm from the needle, which means on the electrode surface when it is used and also 5 mm from the needle. It is at the surface of the liquid. The spectra are measured with the Jobin Yvon spectrometer.

distance mm	connection -	electrode -	I_{RMS} A	temperature K	χ^2 .
He					
2	✗	✗	0.694	430	24
2	✗	✓	0.510	400	24
2	✓	✗	0.450	670	35
2	✓	✓	0.730	850	331
5	✗	✗	0.695	450	48
5	✗	✓	-	-	-
5	✓	✗	0.770	950	25
5	✓	✓	0.730	1000	31
Ar					
2	✗	✗	0.531	400	21
2	✗	✓	0.370	390	15
2	✓	✗	0.450	990	38
2	✓	✓	0.410	790	26
5	✗	✗	0.515	350	19
5	✗	✓	0.380	360	17
5	✓	✗	0.456	950	26
5	✓	✓	0.400	730	30

Table 6.1: Temperature of the OH(A-X) rotational energy for the Helium and Argon plasma jet for different configuration.

The table 6.1 brings together all the temperature for different setup: with or without second electrode and plasma connected or not with the liquid. We can see that one measurement misses for Helium without connection with the liquid but with second electrode. This measurement was difficult to do and the signal was too weak thats is why we would rather to let it free.
If we look at the table, we can notice that for Helium plasma jet without connection with the liquid, the temperature seems to be constant and the root mean square current too. A comparison with the former measurements of the Helium jet only shows that the temperature is around 400 K. It means that there is no change if there is a liquid or not in front of the plume. The cases where the plasma is connected to the liquid is different: the OH(A-X) rotational temperature is much higher. The current is lower with the second electrode than without and the temperature follows the same way which is coherent. More current means more power, so this energy needs to be

dissipated. Actually, we realize after the experiments that the water was quite hot, around 330 K. it means that there is heat transfer between the plasma and the liquid. The current is also constant. About the influence of the electrode, it is difficult to have an idea from the Helium case because of the weak number of measurements in this case. Only one result can be used but the χ^2 which refers to the error is unusually high.

About the Argon plasma jet we can see that without connection with the liquid, the rotational temperature is 100 K less than the previous temperature experiments[3]. Then we can see that the temperature is close to the room temperature. When the plasma is connected with the liquid, the temperature is really high be quite similar along the jet if we compare the temperature from 2 mm to 5 mm. The second electrode plays an important role with Argon plasma jet because the temperature is going lower of 200 K which is a big change. It could be a consequence of the current which is also lower when the second electrode is used. Some energy might is gone in the second electrode and we should also look at the temperature of the second electrode but we did not expect this during the measurements. In the cases where the plasma is no connected and the second electrode is used, the current is lower and the temperature is also lower which is coherent. There is also a fact that we do not expect: when the plasma is not connected the temperature at 2 mm from the needle is around 100 K lower than what we measure for the jet alone[4], but when the plasma is connected, the temperature is really high at 2 mm. It could be the result of some chemical reactions from the aqueous solutions. OH rotational energy might be disturbed by the liquid. From these results but also from the previous one on page 54 the temperatures are higher than the boiling point of water which means that it must be water gas around the plume. This evaporation is notice during the tests because we had to add water to keep the same gap between the liquid surface and the needle. This water might play a role for the OH production. This is a legitimate question because the jet seems to be warmer close to the liquid surface than the needle. But the part of the plasma which is close to the needle should have more energy due to the electric field.

6.6 Complementary investigations

This last chapter may deal with the more interesting part of this report as far as the application is concerned. It is also the part where lots of experiments could be done that is why we need to precise what it should be interesting to do next. First of all, we should try to add Nitrogen and Oxygen in order to compared to the previous tests but also to look into what is happening. It could be necessary to fix the Argon problems measurements due to the charges. A test with liquid with metal particles can help to circulate the charge through the solution. For the future investigation it should be important to look into the spectrum from 400 to 900 nm in order to see if there is some new species. To also have a look at the atomic Oxygen emissions. Then, it could be useful to make the Boltzmann plot an compare with the previous ones.

[3] i.e chapter 5, section 5.4.1, table 5.2 on page 54.

[4] i.e chapter 5, section 5.4.1, table 5.2 on page 54.

Conclusion & Outlook

To conclude, this report is an overview of the results obtained for different diagnostics applied to RF plasma jet. The way that we choose to lead these investigations is progressive. We start to look into the impurity influences by the macroscopic approach. From the pictures we get some information such as Nitrogen induce stability of Argon jet, or Oxygen reduce the jet length. These observations must be link to the plasma chemistry.
The starting point of this project could be the emission spectroscopy investigation. As Descartes said, our senses mislead us and what we learn from the pictures is not exactly what is happened. The spectroscopy helps us to lead the whole investigation because we look into the new species creations but it also explains why the Argon jet is becoming more red when we add Nitrogen. With the emission we also can plan to look into the gas temperature by using OH(A-X) rotational energy level emissions. From this we can make some link with the dissipated plasma power such as Nitrogen induces stability of the power but also of the temperature. The excitation process of Oxygen and Nitrogen are also investigated. The contact between the plasma and the liquid is a quite new experiment for this kind of plasma jet. But the parameter range which can be investigated is huge thus we report some preliminary results such as the influence of the conductivity on the power. It also contains some information about the second electrode influence which should be taken into account for the further investigations.
There are lots of things to look into about this kind of jet. In order to make a link with the medicine application, it will be necessary to measure the absolute concentration of the reactive species. The electron density must be investigated too with the Thomson scattering setup. To be closer to the future applications, it will be important to look into the contact between different plasma mixture and living organisms (bacteria, tissues, blood, ...). For this kind of applications, it must be necessary to have a safe tool which is why a second electrode must be used to keep the current through the patient small. We know that the electrode plays a role on the power and it could be useful to investigate more if the electrode shape can change the plasma. Design some electrodes and test their influence should be interesting, especially for the power. This parameter can also be change to use nanosecond DC-pulsed plasmas and RF DC-pulsed which could reduce the gas temperature but do not influence the chemistry reactions. We can see in the last chapter that the Helium and Argon plasma jet morphology are different when they are connected to a liquid surface. This point should be also investigated because it may drive the future applications. Finally, a fluid mechanics investigation could be done, especially about the viscosity determinations in order to know better how the jet behaves in the air.
The APPJ are a new field of plasma physics which is going to be developed also due to the great potential in medicine applications. Nonetheless, there are still a lot of thing to investigate and the theories which explain these plasma jets have to be developed too.

Bibliography

[1] S. Förster, C. Mohr, and W. Viöl. Investigations of an atmospheric pressure plasma jet by optical emission spectroscopy. *Surface and Coatings Technology*, 200(1-4):827 – 830, 2005. PSE 2004.

[2] Mounir Laroussi and Tamer Akan. Arc-free atmospheric pressure cold plasma jets: A review. *Plasma Processes and Polymers*, 4(9):777–788, 2007.

[3] Cheng Cheng, Zhang Liye, and Ru-Juan Zhan. Surface modification of polymer fibre by the new atmospheric pressure cold plasma jet. *Surface and Coatings Technology*, 200(24):6659 – 6665, 2006.

[4] R Foest, E Kindel, A Ohl, M Stieber, and K-D Weltmann. Non-thermal atmospheric pressure discharges for surface modification. *Plasma Physics and Controlled Fusion*, 47(12B):B525, 2005.

[5] W. R. Bennett, W. L. Faust, R. A. McFarlane, and C. K. N. Patel. Dissociative excitation transfer and optical maser oscillation in ne-*o*2 and ar-*o*2 rf discharges. *Phys. Rev. Lett.*, 8(12):470–473, Jun 1962.

[6] Yixiang Duan, Chun Huang, and Qingsong Yu. Low-temperature direct current glow discharges at atmospheric pressure. *Plasma Science, IEEE Transactions on*, 33(2):328 – 329, apr 2005.

[7] Mounir Laroussi, Claire Tendero, Xinpei Lu, Sudhakar Alla, and Wayne L. Hynes. Inactivation of bacteria by the plasma pencil. *Plasma Processes and Polymers*, 3(6-7):470–473, 2006.

[8] E Castanos-Martanez, M Moisan, and Y Kabouzi. Achieving non-contracted and non-filamentary rare-gas tubular discharges at atmospheric pressure. *Journal of Physics D: Applied Physics*, 42(1):012003, 2009.

[9] M. Teschke, J. Kedzierski, E.G. Finantu-Dinu, D. Korzec, and J. Engemann. High-speed photographs of a dielectric barrier atmospheric pressure plasma jet. *Plasma Science, IEEE Transactions on*, 33(2):310 – 311, apr 2005.

[10] Hideomi Koinuma, Hiroyuki Ohkubo, Takuya Hashimoto, Kiyoto Inomata, Tadashi Shiraishi, Akiharu Miyanaga, and Shigenori Hayashi. Development and application of a microbeam plasma generator. *Applied Physics Letters*, 60(7):816–817, 1992.

[11] H. W. Herrmann, I. Henins, J. Park, and G. S. Selwyn. Decontamination of chemical and biological warfare (cbw) agents using an atmospheric pressure plasma jet (appj). *Physics of Plasmas*, 6(5):2284–2289, 1999.

[12] S E Babayan, J Y Jeong, A Schütze, V J Tu, Maryam Moravej, G S Selwyn, and R F Hicks. Deposition of silicon dioxide films with a non-equilibrium atmospheric-pressure plasma jet. *Plasma Sources Science and Technology*, 10(4):573, 2001.

[13] E Stoffels, Y Aranda Gonzalvo, T D Whitmore, D L Seymour, and J A Rees. A plasma needle generates nitric oxide. *Plasma Sources Science and Technology*, 15(3):501, 2006.

[14] U Fantz. Basics of plasma spectroscopy. *Plasma Sources Science and Technology*, 15(4):S137, 2006.

[15] X R. W. B. Pearse and A. G. Gaydon. *The Identification of Molecular Spectra*. LONDON CHAPMAN & HALL LTD., 3^{rd} edition, 1976.

[16] P. Bicchi. Energy-pooling reactions. *La Rivista del Nuovo Cimento (1978-1999)*, 20:1–74, 1997. 10.1007/BF02879250.

[17] Qian Muyang, Ren Chunsheng, Wang Dezhen, Feng Yan, and Zhang Jialiang. Atmospheric pressure cold argon/oxygen plasma jet assisted by preionization of syringe needle electrode. *Plasma Science and Technology*, 12(5):561, 2010.

[18] Lawrence G. Piper, Michael A. A. Clyne, and Penelope B. Monkhouse. Electronic energy transfer between metastable argon atoms and ground-state oxygen atoms. *J. Chem. Soc., Faraday Trans. 2*, 78:1373–1382, 1982.

[19] David L. King, Larry G. Piper, and Donald W. Setser. Electronic energy transfer from metastable argon (4s3p2,0) to xenon, oxygen and chlorine atoms. *J. Chem. Soc., Faraday Trans. 2*, 73:177–200, 1977.

[20] Peter Bruggeman, Daan C. Schram, Michael G. Kong, and Christophe Leys. Is the rotational temperature of oh(a-x) for discharges in and in contact with liquids a good diagnostic for determining the gas temperature? *Plasma Processes and Polymers*, 6:751–762, 2009.

[21] Irving L. Chidsey and David R. Crosley. Calculated rotational transition probabilities for the a-x system of oh. *Journal of Quantitative Spectroscopy and Radiative Transfer*, 23(2):187 – 199, 1980.

[22] G. H. Dieke and H. M. Crosswhite. The ultraviolet bands of oh fundamental data. *Journal of Quantitative Spectroscopy and Radiative Transfer*, 2(2):97 – 199, 1962.

[23] C Gabriel, S Gabriel, and E Corthout. The dielectric properties of biological tissues: 1. literature survey. *Physics in Medicine and Biology*, 41(11):2231, 1996.

[24] S Gabriel, R W Lau, and C Gabriel. The dielectric properties of biological tissues: 2. measurements in the frequency range 10 hz to 20 ghz. *Physics in Medicine and Biology*, 41(11):2251, 1996.

[25] S Gabriel, R W Lau, and C Gabriel. The dielectric properties of biological tissues: 3. parametric models for the dielectric spectrum of tissues. *Physics in Medicine and Biology*, 41(11):2271, 1996.

[26] B. J. Roth. The electrical conductivity of tissues. In Joseph D. Bronzino, editor, *The Biomedical Engineering HandBook*. CRC Press LLC, second edition edition, 2000.

[27] M. Laroussi and X. Lu. Room-temperature atmospheric pressure plasma plume for biomedical applications. *Applied Physics Letters*, 87(11):113902, 2005.

[28] S. Hofmann and P. Bruggeman. personal communication.